3-10-2014

Thermal Denaturation of Mycobacterium tuberculosis protein Rv0045c monitored by intrinsic tryptophan fluorescence

Lindsey Renee Drake
Butler University

NON-EXCLUSIVE LICENSE FOR USE OF MATERIALS
in the DigitalCommons@Butler University

This non-exclusive License defines the terms for the deposit of Materials in all formats into the digital repository of Materials collected, preserved, and made available through the DigitalCommons@Butler University.

The Contributor hereby grants to Butler University a royalty-free, non-exclusive worldwide License to use, re-use, display, distribute, transmit, publish, republish or copy the Materials, either digitally or in print, or in any other medium, now or hereafter known, for the purpose of including the Materials in the DigitalCommons@Butler University. Butler University will not make any alteration, other than as allowed by this License, to your submission.

Copyright and any other intellectual property right in or to the Materials shall not be transferred by this agreement and shall remain with the Contributor or the Copyright holder if different from the Contributor. Other than this limited License, the Contributor or copyright holder retains all rights, title, copyright and other interest in the Materials licensed.

If the submission contains material for which the Contributor does not hold copyright, the Contributor represents that s/he has obtained the permission of the copyright owner to grant Butler University the rights required by this License, and that such third-party owned material is clearly identified and acknowledged within the text or content of the submission.

If the submission is based upon work that has been sponsored or supported by an agency or organization other than Butler University, the Contributor represents that s/he has fulfilled any right of review or other obligations required by such contract or agreement.

This License shall not authorize the commercial use of the Materials by Butler University or any other person or organization. Butler University will make a good faith effort to ensure that submitted items are used for educational purposes only. All requests for commercial use of submitted materials shall be referred back to the author.

Students making submissions to the DigitalCommons@Butler.edu agree to share their work and waive any privacy rights granted by FERPA or any other law, policy or regulation, with respect to this work, for the purpose of publication.

This agreement embodies the entire agreement of the parties. No modification of this agreement shall be of any effect unless it is made in writing and signed by all of the parties to the agreement.

IN WITNESS WHEREOF, the parties hereto have caused this Agreement to be executed by their authorized agents as of the date stated.

TITLE OF WORK:

Thermal denaturation of Mycobacterium tuberculosis protein Rv0045c monitored by intrinsic tryptophan fluorescence.

CONTRIBUTOR/ADD MY WORK:

Lindsay Drake — 5/6/2014.

Signature **Date**

Lindsay Drake

Printed Name

BUTLER UNIVERSITY (WITNESS):

[signature] — 5/6/14

Signature **Date**

Please sign below if you do not want your work added to the DigitalCommons@Butler.edu.

DO NOT ADD MY WORK:

Signature Date

Printed Name

Rev. 4.22.14 Created 10.25.08

BUTLER UNIVERSITY HONORS PROGRAM

Honors Thesis Certification

Please type all information in this section:

Applicant: Lindsey Renee Drake
(Name as it is to appear on diploma)

Thesis title: Thermal Denaturation of *Mycobacterium tuberculosis* protein Rv0045c monitored by intrinsic tryptophan fluorescence.

Intended date of commencement: May 10, 2014

Read, approved, and signed by:

Thesis adviser(s): Geoffrey C. Hoops — Date: 3/18/14
Geoffrey Hoops

Reader(s): R. Jeremy Johnson — Date: 5/6/14
R. Jeremy Johnson

Judith Harper Morel — Date: 5-13-14
Certified by
Director, Honors Program

For Honors Program use:

Level of Honors conferred: University: Cum Laude

Departmental: Highest Honors in Chemistry

Thermal Denaturation of *Mycobacterium tuberculosis* protein Rv0045c monitored by intrinsic tryptophan fluorescence

A Thesis

Presented to the Department of Chemistry

College of Liberal Arts and Sciences

of

Butler University

In Partial Fulfillment

of the Requirements for Departmental Honors

Lindsey Renee Drake

5 May 2014

Contents

Acknowledgements

Funding for this project was provided by an NSF-TUES Grant, the Butler Summer Institute, and Butler University Chemistry Department. I must thank the entire department for the support and opportunities (both in and out of the classroom) for doing research; my lab mates Jessica Lukowski and Zach Kartje for letting me distract them every day with shenanigans; and my advisor Dr. Geoff Hoops for helping me find all the wrong answers before the right one.

Introduction

The aim of my project was to use intrinsic tryptophan fluorescence to monitor the denaturation pathway of a protein, specifically the *Mycobacterium tuberculosis* enzyme Rv0045c. The larger scientific goal and inspiration for this honors thesis was to use the amino acid residues of a protein to map it's unfolding by thermal denaturation.

Rv0045c

Rv0045c is an esterase from *Mycobacterium tuberculosis*; the organism responsible for the infection and disease tuberculosis[1]. The complete genome sequence[1] of *M. tuberculosis* was determined in 1998. It includes 4,000 genes; among them is Rv0045c, which was identified as a possible dihydrolipoamide acetyl transferase[1]. Rv0045c was later found to be a novel hydrolase of the lipid metabolism cycle in the mycobacterium[2] and to hydrolyze esters, like p-nitrophenyl derivatives[2]. Rv0045c is a member of the alpha/beta fold family; while it shares only little amino acid sequence homology with other such hydrolases, the aforementioned characteristic catalytic residues are preserved[2]. It was speculated from the crystal structure that the binding site includes Gly90, Gln92, Leu155, Ile252, and Phe255; the active residues were identified as the catalytic triade: Asp 178, Ser154, and His309[3]. These residues are highly conserved throughout the alpha/beta fold hydrolase family[3] and thus may be important to the enzyme's activity. The unique structure of Rv0045c offers the opportunity to utilize the enzyme as a drug target, perhaps with an ester containing prodrug. These characteristics attracted the attention of biochemists to the protein; however, only two papers[2,3] have been published on Rv0045c detailing 1.) the initial cloning and characterization as an esterase and 2.) the x-ray crystal structure, respectively.

Denaturation

A new area of inquiry of this protein, Rv0045c, is the determination of unfolded conformations. Denaturation, or unfolding, of proteins seldom occurs in one stage but instead over a range of lower energy conformations. Various agents of denaturation can be used to unfold a protein, such as heat, pH, chelating metallic ions, and chaotropic agents. Thermal stability describes the resistant properties of a protein in its native conformation to heat[4]. Heat affects the weak interactions constructing the tertiary structure of a protein, primarily hydrogen bonds[4]. A protein's conformation remains intact until an abrupt loss of structure occurs over a narrow range when the temperature is increased slowly; the midpoint of this range is called the melting temperature, or T_M[4]. Thus, the T_M value for a protein is a quantitative measurement of when the native conformation of a protein is disrupted. The T_M value could also be defined as the point where the concentration of folded and unfolded proteins is equal[5].

Determining Denaturation

Some methods for determining denaturation are UV CD (ultra violet circular dichroism spectroscopy) and differential scanning fluorimetry. UV CD spectroscopy utilizes circular polarized light to observe signature absorbances of optically active molecules[4]. Far UV CD is the wavelength range that observes secondary structures of proteins like alpha helices and beta sheets. Near UV CD offers information about tertiary structure; however, the spectra cannot be assigned to any specific 3D structure like far UV CD[4]. In general, CD spectra are monitored with changing concentration of detergents, pH, or temperature and used to determine the unfolding pathway of a protein.

Another method for determining the thermal stability of a protein is Differential Scanning Fluorimetry[5] (DSF). Differential scanning fluorimetry (DSF) is a newer high throughput

technique used to monitor thermal unfolding of proteins in the presence of a fluorescent dye[5]. DSF traditionally utilizes a dye (commercially available) that binds to the exposed hydrophobic parts of proteins and whose fluorescence is dependent on the hydrophobic environment. The fluorescence emission can be correlated to denaturation of the protein (more interior hydrophobic pockets open for binding → protein is being unfolded). By using a real-time PCR instrument, measurements can be taken over a matter of hours at discrete temperatures to generate a thermal denaturation temperature curve[5]. The first derivative of the plot of fluorescence versus temperature can be then used to find the midpoint of the curve, or T_M value[5]. Appropriate dyes for DSF include any dye that is highly fluorescent in a non-polar environment[5]. SYPRO orange is a very popular dye because of its high signal-to-noise ratio and high wavelength of excitation, 500nm[5]. This wavelength decreases the likelihood that anything would interfere with the optical properties of the dye.

Tryptophan Fluorescence

To avoid the introduction of an external dye, internal tryptophan fluorescence can be used as the primary indicator of denaturation. Tryptophan, one of the 20 naturally occurring amino acid residues, has the ability to fluoresce[4]. The amino acid tryptophan (figure 1) is the most fluorescent naturally occurring residue; phenylalanine and tyrosine are also weak fluorophores under UV excitation wavelengths[6]. These residues all contain versions of aromatic rings, which have fluorescence potential. Tryptophan's indole ring makes its fluorescence environmentally sensitive. Environmental sensitivity of tryptophan fluorescence can be seen as a blue shift, the emission spectrum being less than the expected 340 nm, when the tryptophan is located in less polar than water environments, like the interior of a folded protein[7]. The most extreme blue shifts have been correlated with increasing nonpolar and densely packed environments[7].

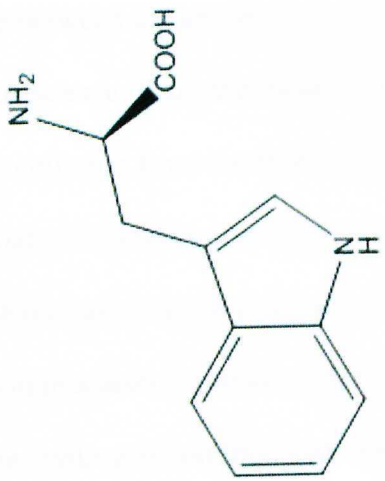

Figure 1. Tryptophan structure

When a fluorescent molecule absorbs energy, it reaches an excited state and then it must release that energy. That release occurs in one of two ways: first, it can fluoresce by emitting a photon of a slightly longer wavelength (lower energy); or secondly, it could participate in nonradiative fluorescence resonance energy transfer (FRET)[4,8,9,10]. In FRET, the excited molecule (called the donor) passes energy directly to a nearby molecule (the acceptor) without emission of a photon, exciting the acceptor; the acceptor can now decay to its ground state by fluorescence[4,8,9,10]. The acceptor's emission has a longer wavelength than both the original exciting light and the emission of the donor[4,8,9,10].

The probability of resonant energy transfer is strongly distance dependent between the donor and acceptor. This relationship allows FRET to act as a spectroscopic ruler, between the distances of 10-100nm[10]. The efficiency of FRET is inversely proportional to the sixth power of the distance between the donor and acceptor[4,8,9,10]. This makes FRET an excellent tool for studying biological molecules because it can be observed in cells as well as in DNA, RNA, or proteins in solution[10].

Because of the close range between the absorbance and emission energies, tryptophans have the ability to quench the fluorescence of another nearby tryptophan. Quenching means a second tryptophan will absorb the emission from the first tryptophan, decreasing the total fluorescence. Quenching is a spatial relationship, which allows conclusions to be drawn on the distance between pairs of tryptophans based on the changing fluorescence signal[4]. Normally, the position of amino acid residues within a protein remains relatively fixed in 3D space due to the rigid, covalently bonded backbone, hydrogen bonding, and other forces; however, during denaturation the tertiary structure is compromised and the spatial relationship between two tryptophans can change. As such, quenching of tryptophan changes and the level of quenching can be measured by fluorescence. If the pairs move closer together, more quenching is observed and vice versa.

Using Intrinsic Tryptophan Fluorescence in Rv0045c

Rv0045c has six tryptophan residues, arranged in internal pairs (figure 2). The fluorescence signal from the tryptophans in Rv0045c is complicated by its multiple tryptophans absorbing, emitting, and quenching their fluorescence. To simplify the fluorescence signal of Rv0045c, multiple tryptophans were knocked out combinatorially by site directed mutagenesis with replacement by phenylalanine using standard molecular biology procedures. The goal of this project is to use the intrinsic tryptophan fluorescence of Rv0045c mutants as a model for following the wild type's thermal denaturation states.

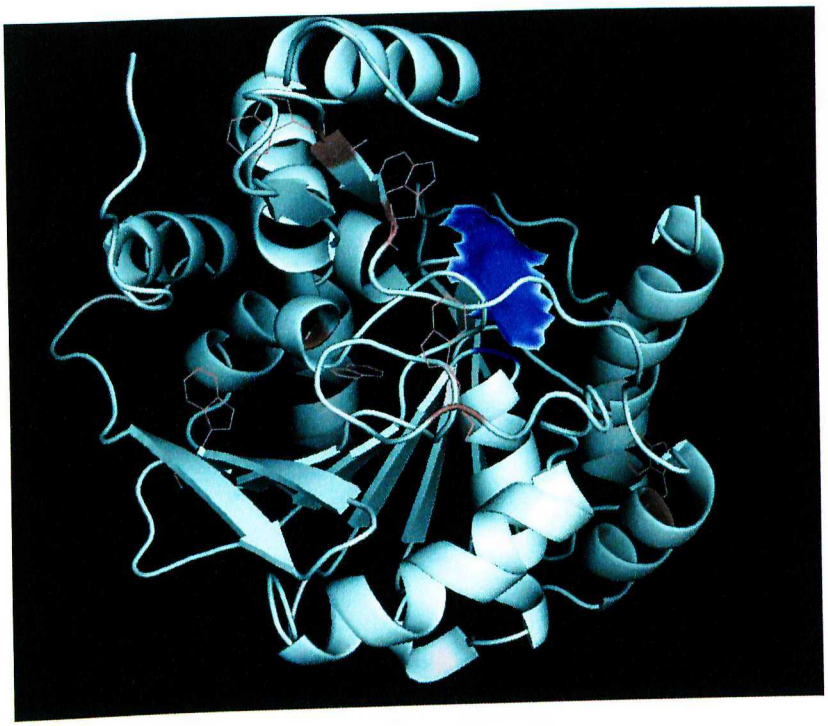

Figure 2. Rv0045c (cartoon) with violet Tryptophan Residues in Stick Form

Rv0045c in cartoon form (Pymol software) from Crystal Structure[2]. Active site, shown as blue surface.

To use a quadruple tryptophan mutant of Rv0045c to observe the wild type's denaturation pathway, the folded structure of Rv0045c needed to remain intact after multiple tryptophan substitutions. Before any intrinsic fluorescence studies were performed, enzymatic assays as well as folding assays were performed to confirm that the tryptophan mutants maintained similar properties to wild type Rv0045c. To ensure the protein was mostly folded, DSF was used to determine T_M values before kinetics were performed at room temperature. A fluorogenic ester substrate was used to measure enzymatic activity using classical Michaelis Menten Kinetics. The esterase Rv0045c hydrolyzed the synthetic ester bonds and released the fluorescein molecule, donated by Lavis Labs Janelia Farms (Figure 3)[11]. This allowed enzymatic measurements to be derived from the appearance of fluorescent product (fluorescein) measured by a fluorimeter. The results will be interpreted and enzymatic values compared to those of the wild type. Single mutant variants of Rv0045c with similar kinetics to wild type will be

preferentially used for further mutagenesis into double mutants. This process will continue sequentially to find the most catalytically viable variants for the quadruple mutant.

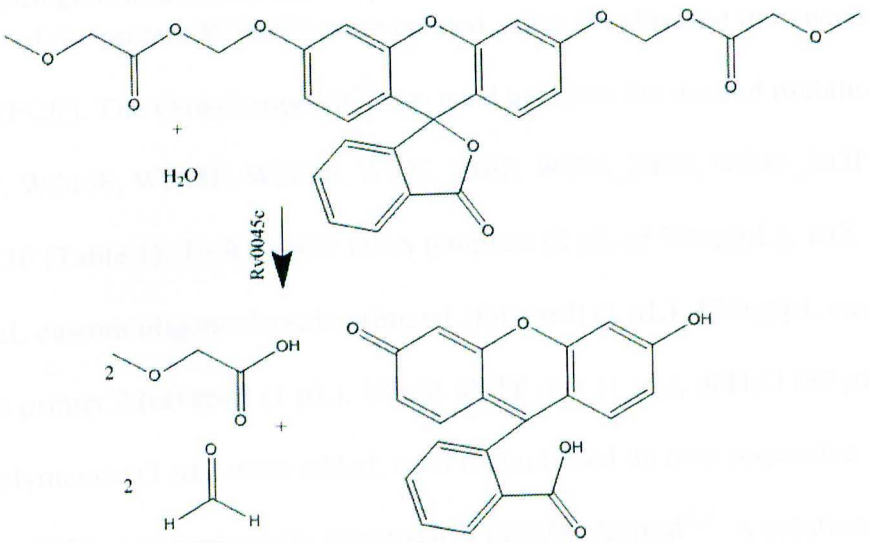

Figure 3. Rv0045c catalyzed hydrolysis of FDMOAME.

The enzyme Rv0045c can hydrolyze the ester bond within the fluorogenic substrate FDMOAME, releasing a hemiacetal product. This product will quickly hydrolyze into fluorescein.

Methods

Site Directed Mutagenesis and Gel Electrophoresis

Mutants of the protein Rv0045c were created using site-directed mutagenesis polymerase chain reaction (PCR). The Quikchange kit[12] was used to create the desired mutations: W78F, W98F, W122F, W246F, W248F, W263F, W122_246F, W246_248F, W246_263F, and W246_248_263F (Table 1). To Rv0045c DNA template (2 µL of 50 ng/µL), 10X reaction buffer (5µL), 125ng/µL custom oligonucleotide primer 1 (forward) (1 µL), 125ng/µL custom oligonucleotide primer 2 (reverse) (1 µL), 10mM dNTP mix (1 µL), ddH_2O (39 µL), and Pfu Turbo DNA Polymerase (1 µL) were added; each mutant used its own respective primers 1 and 2. The template Rv0045c was generously donated in a pET28 plasmid[2, 3]. A solution was made lacking the Pfu Turbo DNA Polymerase to act as a negative control.

To the PCR products, DpnI (1 µL)was added. The resulting mixtures were incubated at 37°C for 1 hour. This experiment utilized DpnI, because it is specific for methylated and hemimethylated DNA[12]; this endonuclease targeted the parental DNA for digestion, selectively leaving mutated DNA in the product mixture.

To observe if the mutagenic PCR was successful, standard Agarose gel electrophoresis procedure was used. To aliquots (10µL) of PCR product, 1% Agarose gel loading dye solution (5µL) were added; the tubes were spun. The gel was loaded with of each sample (12 µL) and of 1 kb DNA ladder (6 µL). The gel was made with 1.5g Agarose dissolved in 100mL of TBE (tris boronic acid EDTA). The mixture was heated to boiling then poured. The gels were run at 100V for 45 minutes in Tris/ Acetic Acid/ EDTA buffer. The gels were stained with ethidium bromide, rinsed, and visualized using UV trans illumination (Appendix A).

Oligonucleotide primers were created by Integrated DNA Technologies, Inc.

Table 1. Oligonucleotide Primers for PCR.

Target Mutant	Oligonucleotide Primer Sequence	Template	Annealing (°C)
W78F	Reverse: 5' CGC AGA GCC GCC AAA GCG CAG CGC CAG CGC GCT GAT GG 3' Forward: 5' CCA TCA GCG CGC TGC GCT TTG GCG GCT CTG CG 3'	Rv0045c	56
W98F	Reverse: 5' CGA CGA TCA CGG TGT CGA AGG TAT GGG CGT TCT G 3' Forward: 5' CAG AAC GCC CAT ACC TTC GAC ACC GTG ATC GTC G 3'	Rv0045c	56
W122F	Reverse: 5' CGT CCT CCC GGA AAG CGG AAT GGC CGT GCC 3' Forward: 5' GGC ACG GCC ATT CCG CTT TCC GGG AGG ACG 3'	Rv0045c	56
W246F	Reverse: 5' CGT CAT AGC GCC ACA CGA AGT TGC CGT TGT CCA G 3' Forward: 5' CTG GAC AAC GGC AAC TTC GTG TGG CGC TAT GAC G 3	Rv0045c	56
W248F	Reverse: 5' GCG TCA TAG CGG AAC AAC CAG TTG CCG TTG TTC A 3' Forward: 5' TGG ACA ACG GCA ACT GGG TGT TCC GCT ATG ACG C 3'	Rv0045c	56
W263F	Reverse: 5' GGC GTC GAC GTC GTC AAA GAG CCC TGC GAA ATC TCC G 3' Forward: 5' CGG AGA TTT CGC AGG GCT CTT TGA CGA CGT CGA CGC C 3'	Rv0045c	56
W122_246F	Reverse: 5' CGT CCT CCC GGA AAG CGG AAT GGC CGT GCC 3' Forward: 5' GGC ACG GCC ATT CCG CTT TCC GGG AGG ACG 3'	W246F	56
W246_248F	Reverse: 5' CGT CAT AGC GGA ACA CGA AGT TGC CGT TGT CCA G 3' Forward: 5' CTG GAC AAC GGC AAC TTC GTG TTC CGC TAT GAC G 3'	W246F	60
W246_248_263F	Reverse: 5' GGC GTC GAC GTC GTC AAA GAG CCC TGC GAA ATC TCC G 3' Forward: 5' CGG AGA TTT CGC AGG GCT CTT TGA CGA CGT CGA CGC C 3'	W246_248F	60
W246_263F	Reverse: 5' GGC GTC GAC GTC GTC AAA GAG CCC TGC GAA ATC TCC G 3' Forward: 5' CGG AGA TTT CGC AGG GCT CTT TGA CGA CGT CGA CGC C 3'	W246F	60

Bacterial Transformation into DH5α

DH5α *E. coli*[13] were used to uptake the pET-28 Vectors (kan resistant) plasmid containing the mutated Rv0045c coding sequence. The kan gene gives bacteria resistance to the antibiotic kanamycin, elimination of non-transformed bacteria can be accomplished by the addition of kanamycin. To QC PCR product (10μL), DH5 α *E.coli* (200 μL) were added and held on ice for 15 min. The transformation mixture was then incubated for 40 s in a 42°C water bath, then put back on ice for 5 min. The reaction was the recovered using of LB media (1 mL) and placed in a shaker at 225 rpm at 37° C for 1 h. The samples were spun down and LB supernatant was removed. Fresh LB media (100 μL) were added to resuspend the pellets. Each suspension was spread onto its own LB-kan plate and kept in an incubator over night at 37°C for colonies to grow. After one week, the colonies were counted and plucked from each mutant. To each colony, LB liquid growth media (3 mL) and 1000x kanamycin concentrated stock (3 μL) were added and the samples were incubated overnight in a 37°C shaker.

DNA Purification

To purify plasmid DNA from the overnight culture, the Miniprep Plasmid DNA purification (IBI Scientific, Peosta, IA, USA , Cat. No. IB47170) protocol was followed. A few changes were made to the procedure[14] including the following variations: in step one the pellets were resuspended using a Vortexer and in step seven DNA was eluted using ddH2O (50 μL) and left standing for 3-5 min on the IBI column.

DNA Concentration

The concentration of the resultant mutants was measured using UV spectroscopy[15] (Appendix C). Spectroscopic measurements were made using a Synergy HI Hybrid Reader. Samples were automatically blanked on water, using a microplate.

Sequence Determination

Sequencing of samples was performed by an external lab: GeneWiz, Inc. Minimum concentration required for sequencing was 10ug/ml. The freeware program BioEdit was used to compare the sequences of the mutants to the wild type Rv0045c protein for the desired point mutations.

Protein Overexpression and Purification

Rv0045c protein variants were overexpressed in *E. coli* as an N-terminal 6xHis-tag fusion using a bacterial expression plasmid (pET28a) containing the Rv0045c gene from *M. tuberculosis* between the BamHI and XhoI restriction sites as previously described[2]. This bacterial plasmid (pET28-Rv0045c) was transformed into *E. coli* BL21 (DE3) RIPL cells[16] (Agilent, La Jolla, CA) using an analogous procedure to the DH5α transformation. A saturated overnight culture of *E. coli* BL21 (DE3) RIPL (pET28-Rv0045c) in LB media containing kanamycin (40 μg/mL) and chloramphenicol (30 μg/mL) was used to inoculate LB-media (250 mL) containing kanamycin (40 μg/mL) and chloramphenicol (30 μg/mL) and the bacterial culture was grown with constant shaking (225 rpm) at 37 °C. When the OD_{600} reached 0.6 – 0.8, the temperature of the culture was decreased to 16 °C and isopropyl β-D-1-thiogalactopyranoside (IPTG) was added to a final concentration of 1.0 mM. Protein induction proceeded overnight (~16-20 hours) at 16 °C. Bacterial cultures were collected by centrifugation at 6,000 × g for 10 min at 4 °C. The bacterial cell pellet was resuspended in PBS (5 mL) and stored at -20 °C.

To disrupt the bacterial cell wall, lysozyme (50 mg; Sigma-Aldrich) and 10X Bug Buster solution (700 µL; EMD Millipore) were added to the thawed cell pellet; cell lysis proceeded on an orbital shaker for 1 h at 4 °C. To remove insoluble cell material, lysed cells were centrifuged at 10,000 x g for 10 min at 4 °C. Ni-NTA agarose (600 µL; Qiagen, Valencia, CA) was added to the soluble fraction and allowed to incubate at 4 °C for 2-4 h. The resin was washed three times with PBS containing increasing concentrations of ice-cold imidazole (20 mL each of PBS containing 10 mM imidazole, 25 mM imidazole, or 50 mM imidazole) and recollected by centrifugation at 2000 × g for 2 min at 4 °C. Rv0045c variants were eluted in PBS containing 250 mM imidazole (2 mL) and dialyzed (10K MWCO; Pierce, Rockford, IL) against PBS overnight at 4 °C with constant stirring.

Concentration and Purity of Rv0045c Variants

The purity of Rv0045c variants were confirmed by SDS–PAGE on a 4–20% gradient gel (Novex-LifeTechnologies) visualized with colloidal Coomassie brilliant blue (Appendix B). The concentration of Rv0045c was determined by measuring the absorbance at 280 nm and converting to molarity units with the respective extinction coefficients: $\varepsilon^{280} = 30480\ M^{-1}\ cm^{-1}$ for single mutants, $\varepsilon^{280} = 24980\ M^{-1}\ cm^{-1}$ for double mutants, and $\varepsilon^{280} = 19480\ M^{-1}\ cm^{-1}$ for triple mutants (Appendix C). The significant changes in the extinction coefficients are expected, because tryptophan residues are some of the biggest absorbers in the protein and removing them lowers the extinction coefficient. Extinction coefficients were calculated from the theoretical amino acid sequence using the ProtParam online proteomics on the ExPASy web site (http://web.expasy.org/protparam).

Differential Scanning Fluorimetry Thermal Stability Assay

Samples were diluted to a concentration of 0.3 mg/mL in PBS with 0.002X Sypro Orange (1µL) (Invitrogen, Burlington, ON, Canada, Cat. No. S-6650). Three replicates were completed

for each mutant. The plate was read in the Bio-rad C1000 Thermocycler with CFX96 Real-time System. The samples were heated from 15 °C to 80 ° C at a rate of 1 °C/min. Data was analyzed using Bio-Rad CFX Manager software.

Enzyme Kinetics

Mutants were diluted to 150 μg/mL in phosphate buffered saline containing 0.1 mg/mL acetylated bovine serum albumin (PBS+BSA). Initially in a PCR plate, the top seven wells (A-G) in columns 1-10, disregarding 7, contained 120μL of PBS+BSA. The bottom row (wells H) in those nine columns were filled with PBS+BSA (178 μL) and 10mM fluorogenic substrate (1.8μL) (FDMOAME). A substrate dilution series was set up in eight wells of nine columns of a PCR plate, decreasing by 1/3 from well H to well A. The dilution series was made by adding 60μL of well H to well G, and subsequently up the column to well A. To a black assay plate, the samples (95μL) were moved from the PCR wells to the corresponding black assay plate wells. A fluorescein standard was made in column 7 by adding 300 nM fluorescein solution (240μL) to well H, PBS+BSA buffer (120μL) in wells A-G, transferring half from well H to well G, and subsequently up the column to well A. To columns 1-3,4-6, and 8-10, various enzyme dilutions (5μL) were added. Substrate concentrations ranged from 100 μM to 0.0457.

The micro plate was analyzed on a Synergy H1 Hybrid Reader. Fluorescence data were collected at an excitation of 485nm and emission of 520nm for 5 min, at an interval of 15s. The relative fluorescence data for each well at each time interval was exported to Microsoft Excel. Column 7 with the known concentration of the fluorescein standard was used to create a best fit line correlating fluorescence units with concentration. The best fit line equation was used on the raw fluorescence data of the other wells to find corresponding product concentrations at each time point. The slope was then taken of the product concentration against time interval (in

seconds) to calculate the initial velocities of the enzyme catalyzed reaction. For each triplicate, the velocities for each concentration of substrate were averaged. The average initial velocity and substrate concentration were fitted to the Michaelis-Menten equation using Origin 6.1 software. From the fitting of this equation, the K_M and V_{max} values were calculated. Using these values in Excel, the V_{max} value was divided by enzyme concentration to determine the k_{cat}. K_M and k_{cat} values that are reported for each enzyme variant.

Thermal stability by IF

Intrinsic fluorescence was monitored over 28 reads in the Synergy H1 hybrid reader, from room temperature to ~60°C, collecting every degree up to 45°C and every three degrees from 45- 60°C. A triplicate of enzyme samples were (15ng) each dissolved in 1X PBS buffer, along with a blank as a control were loaded into the 96 well black assay plate along with (100µL; wells D6, D7, E6, and E7). Starting at room temperature, the fluorescence measurement was taken at excitation 280nm, emission 340nm. Data recorded included maximum emission wavelength and maximum relative fluorescence. After 45°C, the Synergy instrument ejected the plate and it was placed in the Thermal Protein Denaturationator 2000, gen 3 (figure 4), and heated for 90 seconds up to 47°C. The plate was inserted back into the Synergy instrument which prompted the instrument to take another read. This procedure was repeated five more times at increasing temperatures (varied upon trial).

Individual run data, including emission wavelength, maximum fluorescence absorbance, and temperature were exported to Excel. The fourth well (E7) consisting of only solvent was used to correct background fluorescence. The average of the triplicates corrected for background fluorescence was calculated. Relative fluorescence units were plotted against temperature in

Origin 6.1 software. The data was fit to a single sigmoidal curve (Appendix E). Best fit lines were used to approximate T_M's.

Figure 4. Intrinsic Fluorescence Method

Shown far left is the variometer which controls the amount of current passing to heating mantel inside Styrofoam oven. Far right is Synergy H1 Hybrid reader. The oven is composed of a heating mantel in the bottom with a tin foil shelf resting approximately 4 inches above it. The samples in a black well 96 well assay plate rest on the tin foil shelf. The samples are inserted and removed through the door carved into the front. A thermometer is pushed through the Styrofoam top, the end resting approximately 1 inch above the sample wells.

Results and Discussion

The goal of this project was to use the intrinsic tryptophan fluorescence of Rv0045c mutants as a model for following the protein's thermal denaturation states. The observe the folding pathway of Rv045c by intrinsic tryptophan fluorescence, the folded structure of Rv0045c needed to remain intact after multiple tryptophan substitutions. To begin to prepare the necessary quadruple tryptohan mutant for IF studies, preliminary folding stability and kinetic analysis were performed on all six single tryptophan to phenylalanine mutants.

Successful preparation of single tryptophan mutants: W78F, W98F, W122F, W246F, W248F, and W263F.

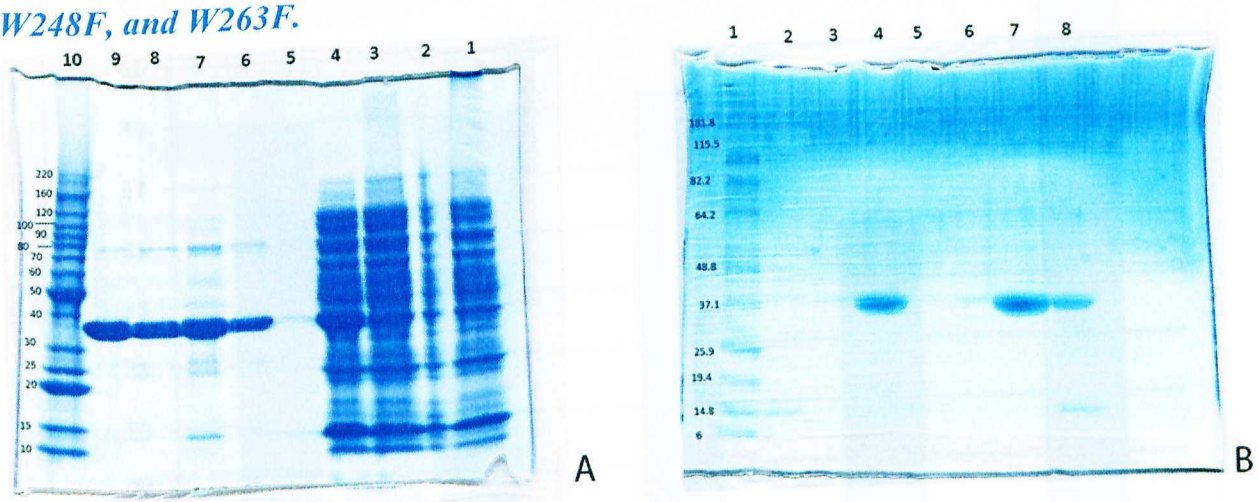

Figure 5. SDS PAGE of single mutants

The 4-20% Agarose gels were run at 150V for two hours in 1X Tris Glycine buffer. It was visualized using SimplyBlue **A**. SDS PAGE Analysis of Rv0045c Mutants. Lane 1: W98F flow-through. Lane 2: W122F flow-through. Lane 3: W246F flow-through. Lane 4: W248F flow-through. Lane 5: W122F second wash. Lane 6: W98F pure. Lane 7: W122F pure. Lane 8: W246F pure. Lane 9: W248F pure. Lane 10: Benchmark Protein Ladder. **B**. SDS PAGE Purification: Lane 1: MW marker. Lane 2: Wash one of W78F. Lane 3: Wash three of W78F. Lane 4: Pure W78F. Lane 5: Wash one of W263F. Lane 6: wash three of W263F. Lane 7: Pure W263F. Lane 8: Pure W122_W246F.

The preparation of all single mutant plasmids, W78F, W98F, W122F, W246F, W248F, and W263F, was confirmed first in ethidium bromide gel staining which indicates the success of the PCR reaction (Appendix A). The successful preparation of mutations was confirmed by DNA

sequencing, performed by an external source: GeneWiz Inc. The protein overexpression and purification was confirmed by SDS PAGE (figure 5). In gel A, lanes 6, 7, 8, and 9 respectively show the relative purity of variants W98F, W122F, W246F, and W248F. The major bands are large and near the expected size, 36 kD, with lighter bands associated with other protein impurities. Similarly, the purity of variants W78F and W263F is shown by lanes 4 and 7 of gel B.

Four mutants, W122F, W246F, W248F, W263F, are suitable for further mutagenesis.

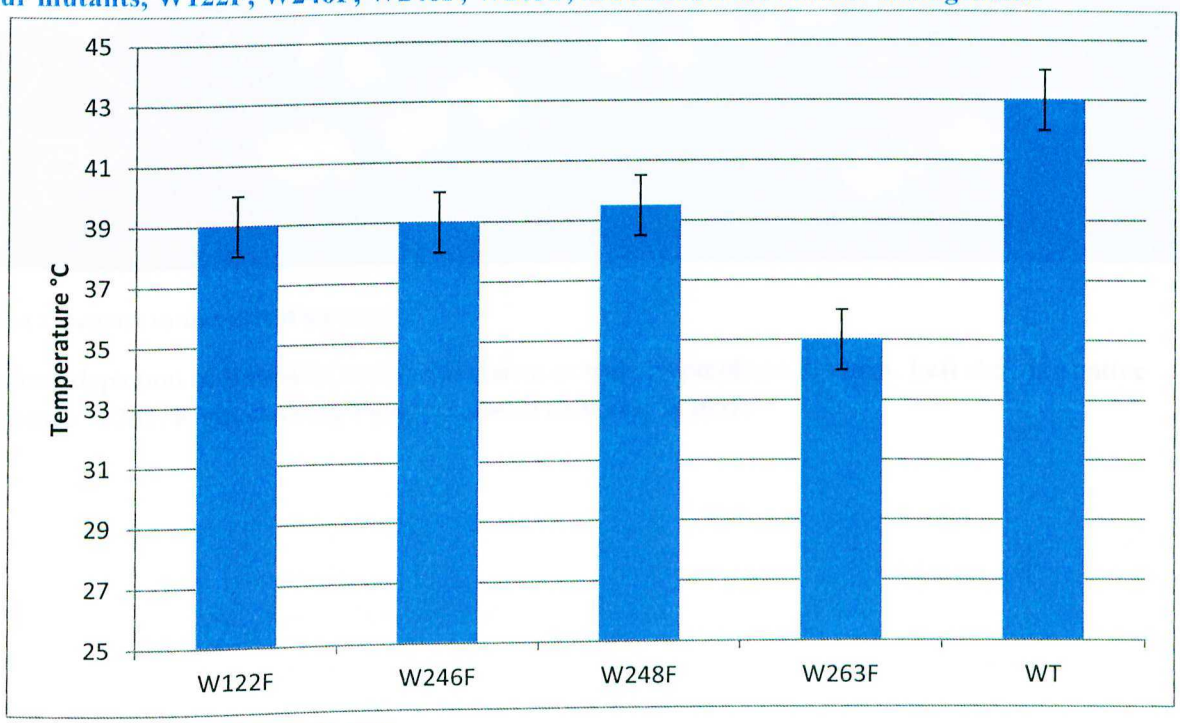

Figure 6. Folding Stability of Single Mutants

The folding stability was determined by Differential Scanning Fluorimetry using the dye SYPRO orange. Melt curves and first derivatives shown in Appendix D.

The folding stability of the proteins was important for determining suitability for the kinetic assays. The enzyme variants were all found to be stable at room temperature, 25°C, similar to wild type (Figure 6). The mutations do however destabilize the folded stability of Rv0045c. Each of the single mutants have a lowered T_M compared to wild type, but are completely folded at 25°C. W263F is the most destabilizing mutation. In the crystal structure of

Rv0045c (figure 7), W263F is located in an alpha helical section of Rv0045c. Mutations within the helix are likely destabilizing to the enzyme. Because the Rv0045c variants were conformationally stable at room temperature, Michaelis-Menten kinetics could be performed for all single mutants at 25°C.

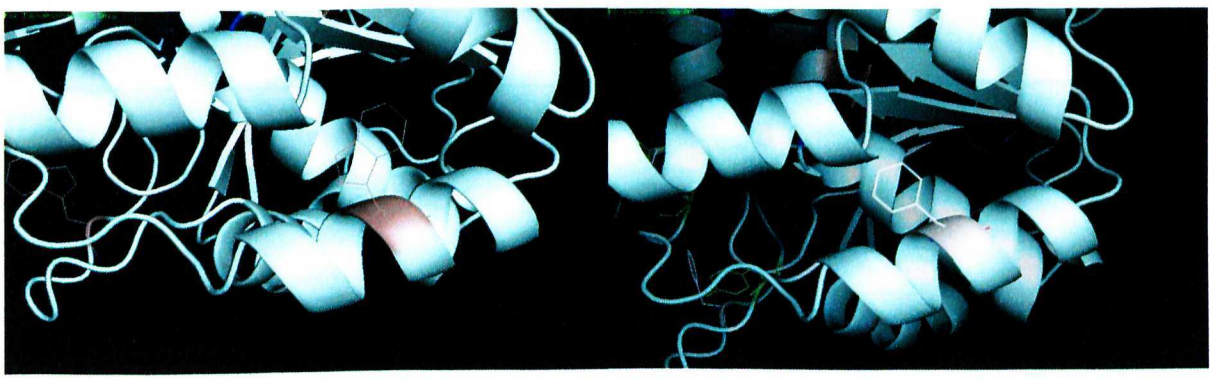

Figure 7. Rv0045c variant W263F (cartoon)

Cartoon depiction of Rv0045c, active site shown in blue, tryptophans in violet. Left showing native sequence W263. Right showing Pymol modeled mutation W263F.

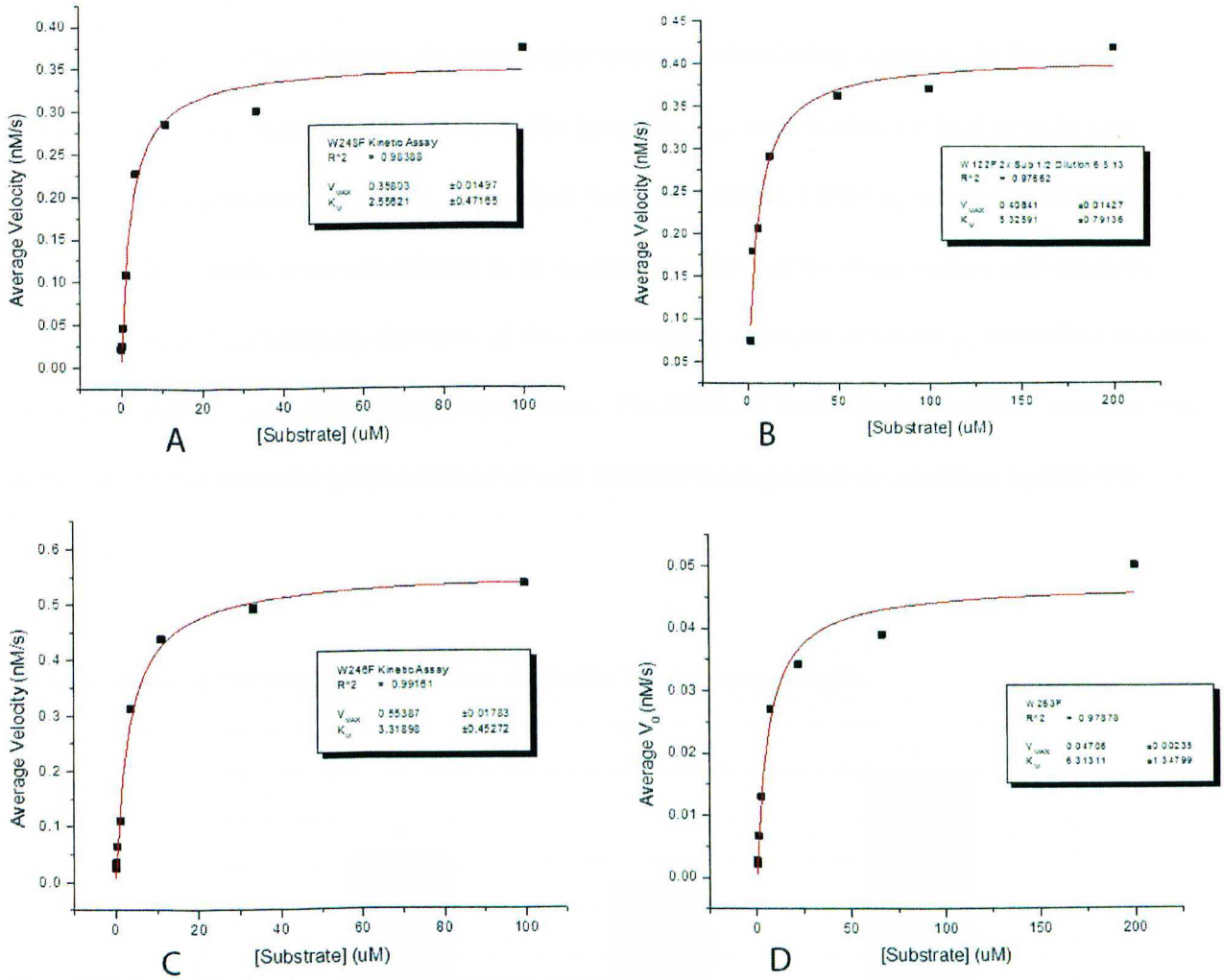

Figure 8. Michaelis-Menten Curves of Successful Single Mutants

Average velocity versus substrate concentration fit to Michaelis-Menten equation in Origin 6.1. V_{max} and K_M values reported from the equation fitting. **A**. W248F. **B**. W122F. **C**. W246F. **D**. W263F.

Table 2. Michaelis-Menten Values of Successful Single Mutants

Mutant	k_{cat} (1/s)	k_{cat} error	K_M (μM)	K_M error	k_{cat}/K_M ($M^{-1}s^{-1}$)
W248F	0.001697	8.04E-06	2.556	0.4716	664
W122F	0.001936	9.18E-06	5.32	0.79136	363
W246F	0.002625	1.24E-05	3.318	0.015725	791
W263F	0.00515	2.44E-05	6.31	1.347	816
Wild Type*	0.011142	0.00062	2.595	0.63631	4292.976

*Provided by J. Lukowski.

The mutants W122F, W246F, W248F, and W263F, exhibited Michaelis-Menten like kinetics (figure 8). Their kinetic characteristics were observed using substrate FDMOAME (figure 3). The resultant calculated values for turnover, k_{cat} were within 10 fold of wild type (table 2). The tightness of binding, K_M, values were also within 2 fold to wild type (table 2). These single mutants were considered to be similar to wild type by these values and catalytic efficiency, k_{cat}/ K_M (Table 2). Because of this similarity in catalytic efficiency, these four mutants were determined viable for further mutagenesis. The DNA of these single Rv0045c variants was then used as the basis for another round of site directed mutagenesis to combine tryptophan mutations.

Two mutants, W78F and W98F, are not viable for further mutagenesis.

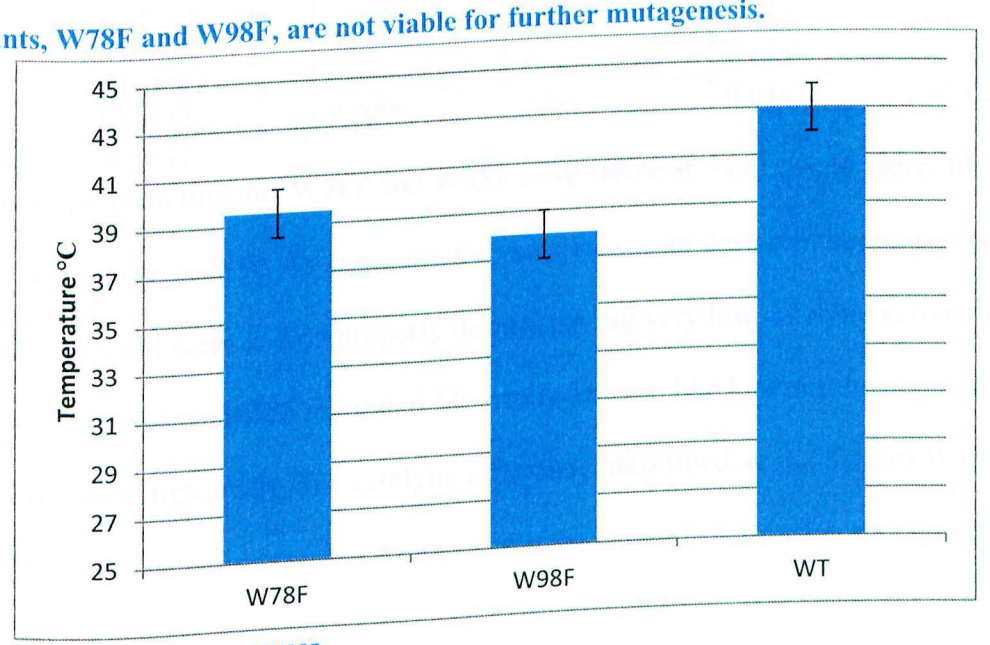

Figure 9. Folding Stability of W78F and W98F

The folding stability was determined by Differential Scanning Fluorimetry using the dye SYPRO orange. Melt curves and first derivatives shown in Appendix D.

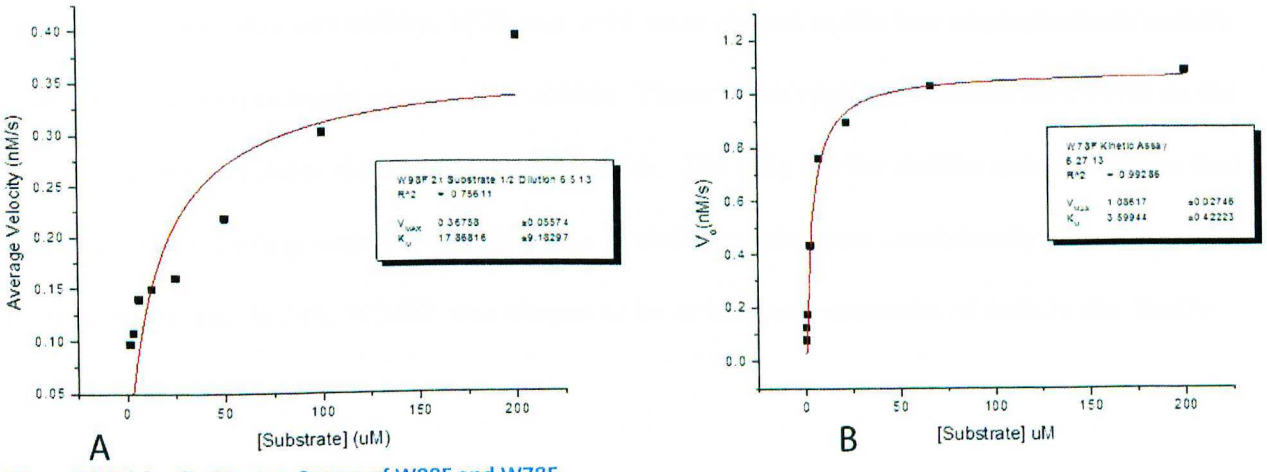

Figure 10 Michaelis-Menten Curves of W98F and W78F

Average velocity versus substrate concentration fit to Michaelis-Menten equation in Origin 6.1. V_{max} and K_M values reported from the equation fitting. **A**. W98F. **B**. W78F.

Table 3. Michaelis-Menten Values of W78F and W98F

Mutant	k_{cat} (1/s)	k_{cat} error	K_M (μM)	K_M error	k_{cat}/K_M ($M^{-1}s^{-1}$)
W78F	0.000223	1.06E-06	3.1	0.422	61
W98F	0.001742	8.26E-06	17.9	9.182	97.49
Wild Type*	0.011142	0.00062	2.595	0.63631	4292.976

*Provided by J. Lukowski

The tryptophan mutants W78F and W98F were stable at room temperature, like the other four single mutants (Figure 9). As expected, the mutations were destabilizing to the enzyme. Interestingly, they did seem to fold properly despite having very low catalytic activity compared to wild type. Only variant W78F exhibited Michaelis-Menten like kinetics; however, not to a desirable efficiency (figure 10). The catalytic efficiency, described as k_{cat}/K_M, for W78F, was at least 10-fold lower than wild type and determined to be unviable for further mutagenesis (table 3).

Variant W98F did not exhibit Michaelis-Menten like kinetics. The fit in plot A of figure 9 reveals the R^2 for the hyperbolic fit is only 0.756. Realistically the values generated from this curve fit are not usable and do not reflect the activity of the enzyme. Because of this, W98F was determined to not be viable for further mutagenesis.

In light of this unviability, W78 and W98 were chosen as the two tryptophans to remain intact in the final quadruple mutant of Rv0045c. These two tryptophans would then serve as the quenching pair to follow the unfolding of Rv0045c. The plan for the double mutants was to find the most viable pairing with W246F. Because W246F was the most catalytically efficient in the pairing W246 and W248, W246F was chosen to be at least one mutation of each in the double mutants.

Creation of stable double mutants W122_246F, W246_248F, and W246_263F was successful. Variant W246_248F is most viable for further mutagenesis.

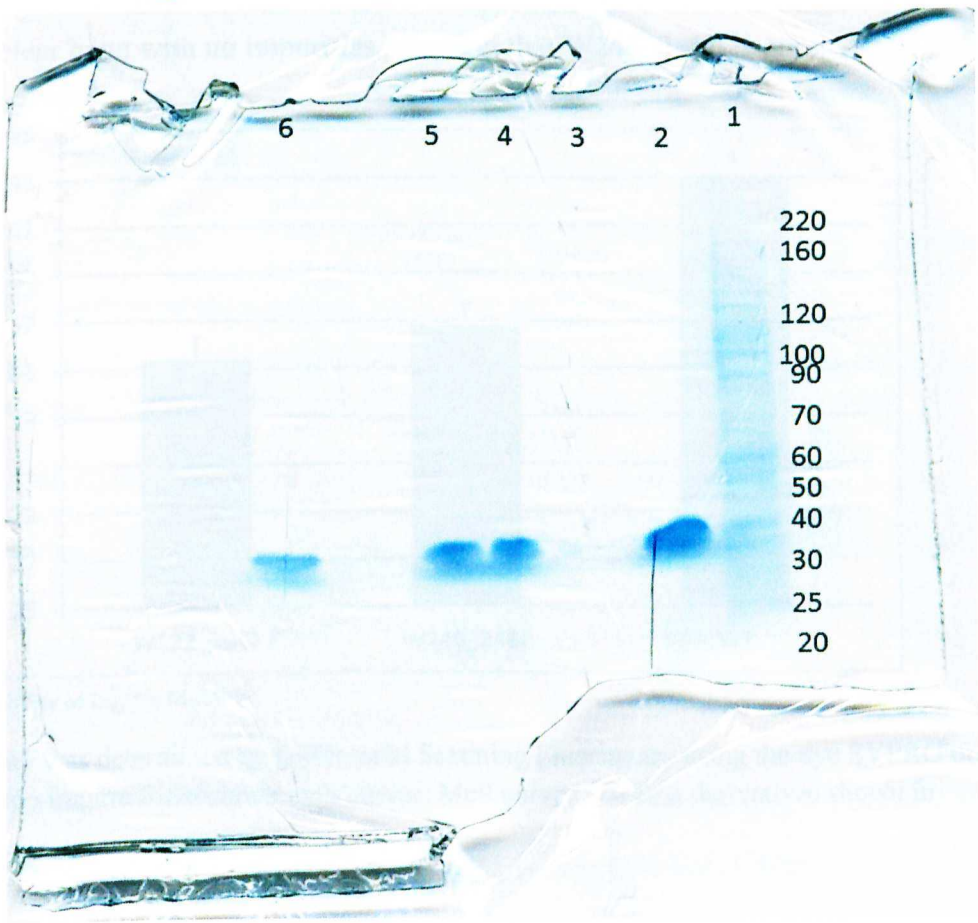

Figure 11. SDS PAGE of Double and Triple Mutants

SDS PAGE.4-20% Tris Glycine gel run in tris glycine buffer at 150V for two hours. Lane 1: MW marker. Lane 2: W122_246F. Lane 3: blank. Lane 4: W246_248F. Lane 5: W246_263F. Lane 6: W246_248_263F.

The preparation of three double mutant plasmids, W122_246F, W246_248F, and W246_263F, was confirmed first in ethidium bromide gel staining which indicates the success of the PCR reaction (Appendix A). The successful mutation was confirmed by DNA sequencing, performed by an external source: GeneWiz Inc. Overexpression and purification of double Rv0045c mutants was confirmed by SDS PAGE analysis. As seen in lane 5 (Figure 11), a dark band of W246_263F Rv0045c was present around 36 kD. There are light bands around it showing that it is not completely pure. Lane 2 shows a band present of W122_246F with a light band slightly below, associated some protein contaminant (an impurity left from the washes). Lane 4 shows a clear band with no impurities, showing that W246_248F is pure.

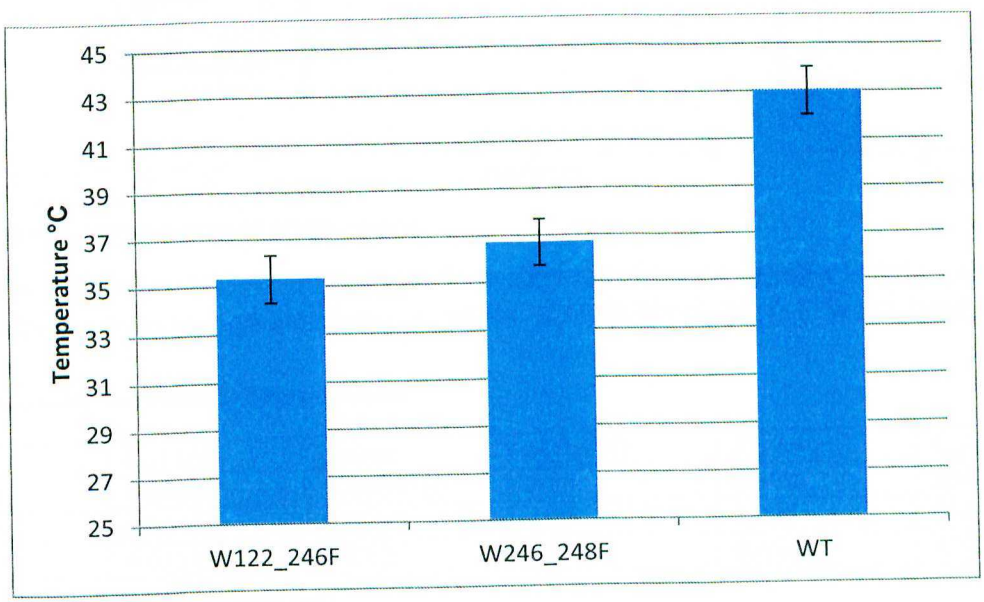

Figure 12. Folding Stability of Double Mutants.

The folding stability was determined by Differential Scanning Fluorimetry using the dye SYPRO orange. W246_263F was too impure for accurate melt curves. Melt curves and first derivatives shown in Appendix D.

Differentially scanning fluorimetry of the double mutants showed that the variants are still folding properly at room temperature (Figure 12). Compared to the single variants W122F and W246F with T_M's of 39°C, the double mutant variant W122_246F is only slightly

destabilized. Similarly, the double mutant W246_248F is still similar to its parent single variants W246F and W248F with respective T_M's of 39°C and 40°C. Interestingly, the additional double mutant is less if not just as destabilizing as a single mutation to Rv0045c. Mutant W246_263F yielded no usable melt curves from DSF. The impurities, judging clean band from the SDS PAGE gel, are most likely imidazole from the washes. This impurity drastically changes the melt curve of the enzyme, rendering the curve nearly flat with no definite melt peak in the first derivative graph.

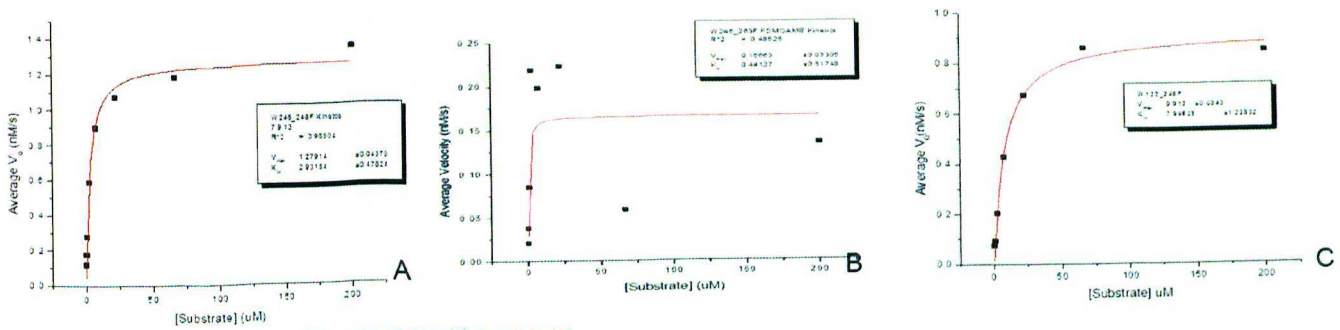

Figure 13. Michaelis- Menten Curves of Double mutants

Average velocity versus substrate concentration fit to Michaelis-Menten equation in Origin 6.1. V_{max} and K_M values reported from the equation fitting. **A**. W246_248F, **B** W246_263F, **C** W122_246F.

Table 4. Michaelis-Menten Values of Double Mutants

Mutant	k_{cat} (1/s)	k_{cat} error	K_M (μM)	K_M error	k_{cat}/K_M ($M^{-1}s^{-1}$)
W246_248F	0.00606	2.87299E-05	2.93	0.478	2068
W122_246F	0.00433	2.05E-05	7.95	1.228	544.5
Wild Type*	0.011142	0.00062	2.595	0.63631	4292.976

*Provided by J. Lukowski.
**W246_263F did not generate any usable values.

Kinetically, two of the double mutants still exhibit Michaelis-Menten like activity (Figure 13). Panel B shows a poor fitting curve of W246_263F which does not exhibit Michaelis-Menten kinetics. This may be attributed to impurities associated with W246_263F, or that truly this mutation is detrimental to the activity of the enzyme. Considering that there was no usable melt

curve from DSF, the protein was likely unfolded after its creation and that is why there is no Michaelis-Menten like kinetics or folding stability.

Variants W122_246F and W246_248F mutants were as viable as the four single most viable mutants W122F, W246F, W248F, and W263F according to the k_{cat}/K_M values. The double mutant with the highest catalytic efficiency is W246_248F (table 4). Because of this efficiency, and the convenience of the pair FRET pair W246 and W248 being knocked out, this mutant was chosen to be the platform for further mutagenesis. Interestingly, W246_248F is more catalytically efficient than any of the single mutants.

Successful creation of triple mutant: W246_248_263F.

The preparation of the triple mutant W246_248_263F was confirmed first in ethidium bromide gel staining which indicates the success of the PCR reaction (Appendix A). The successful mutation was confirmed by DNA sequencing, performed by an external source: GeneWiz Inc. Overexpression and purification of the triple mutant was confirmed by SDS PAGE analysis (Figure 11). Lane 6 of the gel shows the expected size of the Rv0045c variant. The band is not completely sharp, indicating impurities left from the wash.

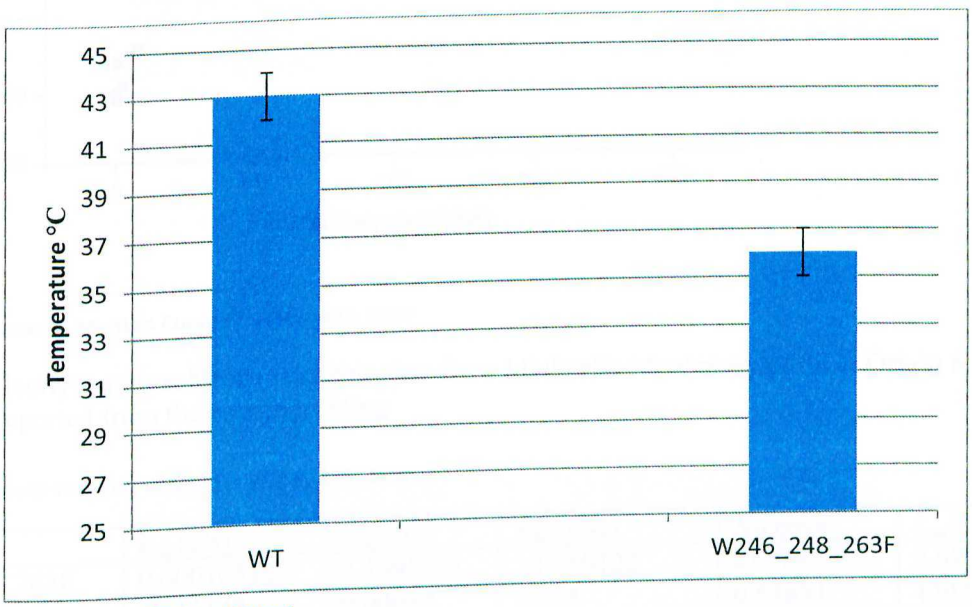

Figure 14. Folding Stability of Triple Mutant

The folding stability was determined by Differential Scanning Fluorimetry using the dye SYPRO orange. Melt curves and first derivatives shown in Appendix D.

The triple mutant was found to be properly folded at room temperature (Figure 14). This is promising, as it shows that even three mutations on residues do not detrimentally alter Rv0045c. It was expected, as the single and double mutants destabilized the enzyme, that three mutations would be destabilizing as well. Comparably, W246_248_263F's T_M is the same as double mutant W246_248F (Figures 12 and 14). Seemingly, the additional third mutation did not affect the stability of the protein as much as the initial two mutations. Based on this stability, W246_248_263F could be a good candidate for further mutagenesis.

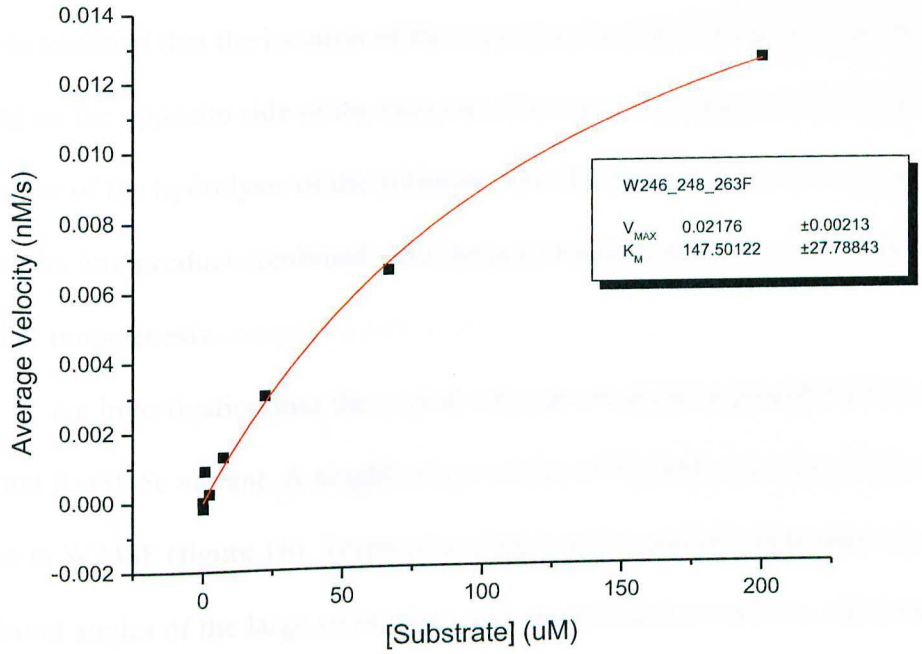

Figure 15. Michaelis-Menten Curve of W246_248_263F

Average velocity versus substrate concentration fit to Michaelis-Menten equation in Origin 6.1. V_{max} and K_M values reported from the equation fitting.

Table 5. Michaelis-Menten Values for W246_248_263F

Mutant	k_{cat} (1/s)	k_{cat} error	K_M (μM)	K_M error	k_{cat}/K_M ($M^{-1}s^{-1}$)
W246_248_263F	0.000103128	2.139E-05	147.50122	27.788	0.699166841
Wild Type*	0.011142	0.00062	2.595	0.63631	4292.976

*Provided by J. Lukowski.

The triple mutant variant of Rv0045c, W246_248_263F, does not however exhibit well behaved Michaelis-Menten like kinetics (Figure 15). Despite being folded at room temperature like the other mutants created, the triple mutant was not stable enough to hydrolyze as efficiently as wild type. Interestingly, the addition of a second mutation to the enzyme was just as detrimental as the primary mutations; however, it seems the addition of a third mutation is not as destabilizing in Rv0045c. It may be due to the location of these particular residues all being in the same general area of the protein.

The enzyme shows significantly less tightness of binding, the K_M being 147 μM (table 5). It was assumed that the location of the mutations would not interfere greatly with the active site, being on the opposite side of the enzyme. The lower k_{cat} value would indicate a much slower turnover of the hydrolysis of the substrate into fluorescein product. The slow turnover of substrate into product combined with the poor binding affinity makes this enzyme unviable for further mutagenesis.

An investigation into the crystal structure revealed a possible steric hindrance in the triple mutant Rv0045c variant. A neighboring residue of W248F, tyrosine 250 is modeled to be very close to W248F (figure 16). Tryptophan 248 is at the end of a beta sheet as well. Because of the different angles of the large tryptophan and phenylalanine residues, this beta sheet may be compromised, because of steric interactions with its neighboring tyrosine Y250. It is important to note that the view in a crystal structure is stagnant and equivocal to a snap shot. In the biologically active form of the enzyme this steric hindrance may not be occurring.

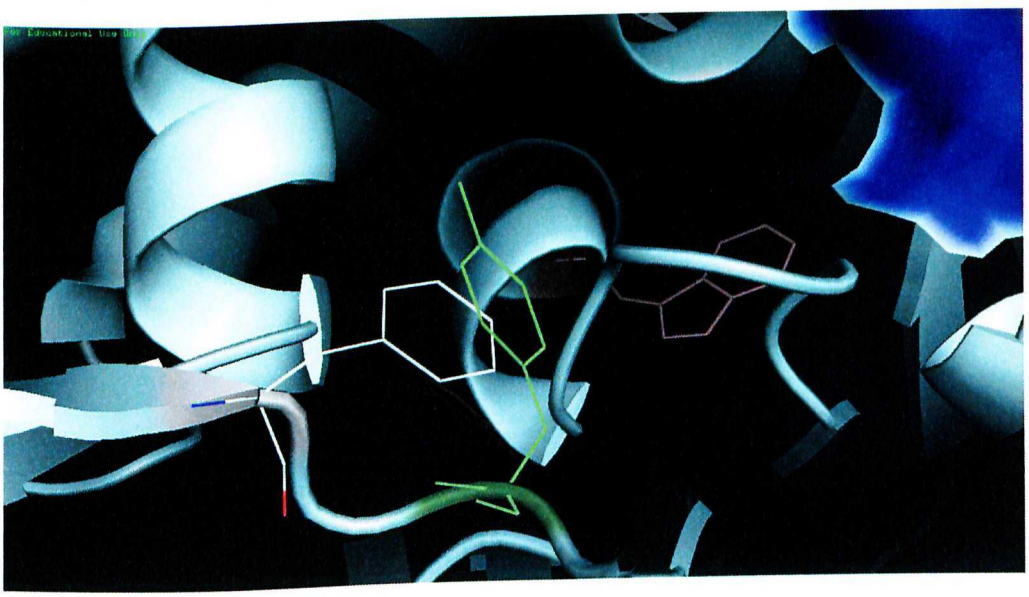

Figure 16. Rv0045c (cartoon) close up of W248F and Y250

Cartoon depiction of Rv0045c, active site shown in blue, tryptophans in violet. Close up of W248F and neighboring tyrosine Y250.

Rv0045c variant W246_248_263F's lack of enzymatic activity prevents the further mutagenesis of this particular Rv0045c variant. The experimental design is still viable with different variants. A more stable triple mutation would most likely be W122_246_248F. The quadruple mutant target of W122_246_248_263F is not realistic, however, considering the instability associated with W263F. The reevaluation of secondary structure agrees with the redirection of the quadruple mutant target.

Intrinsic Fluorescence of Rv0045c Variants is measurable.

To develop the intrinsic fluorescence method, the protocol described in the Materials and Methods was performed on most of the mutants; the concerns about the integrity of W246_263F prevented the assay from being completed on this mutant. Intrinsic fluorescence for all mutants remained in a similar range, with W122_246F being the only significant difference. All sigmoidal curves were observed with emissions at 314nm and an overall decrease in fluorescence. The general hypothesis that there would be an increase in quenching from denaturation is supported by all IF assays. Variants followed either single phase or biphasic denaturation curves; the former having only folded and unfolded states and the latter showing a potential third unfolded state.

IF Thermal Assays of Single Mutant Rv0045c Variants W78F and W263F are single phased.

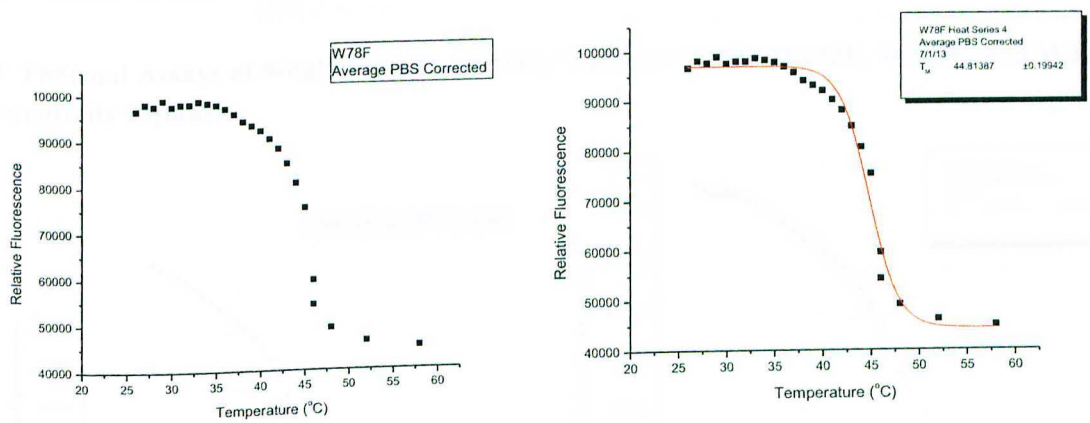

Figure 17. IF Curve of W78F

T_M value by best fit found to be 44°C. Excitation at 280nm and maximum fluorescent emissions at 314nm were measured.

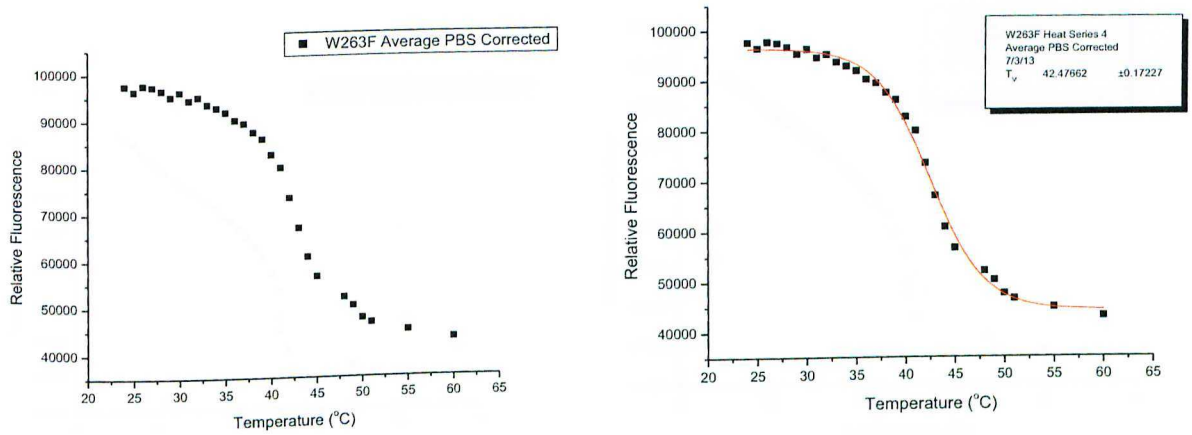

Figure 18. IF Curve of W263F

T_M by best fit found to be 42°C. Excitation at 280nm and maximum fluorescent emissions at 314nm were measured.

The variants W78F (figure 17) and W263F (figure 18) were well fitted to a single sigmoidal curve, indicating the variants are undergoing one stage of denaturation. The T_M values reported accurately describe the data for both curves.

IF Thermal Assays of Single Mutant Rv0045c Variants W98F, W122F, W246F, and W248F are Potentially Biphasic.

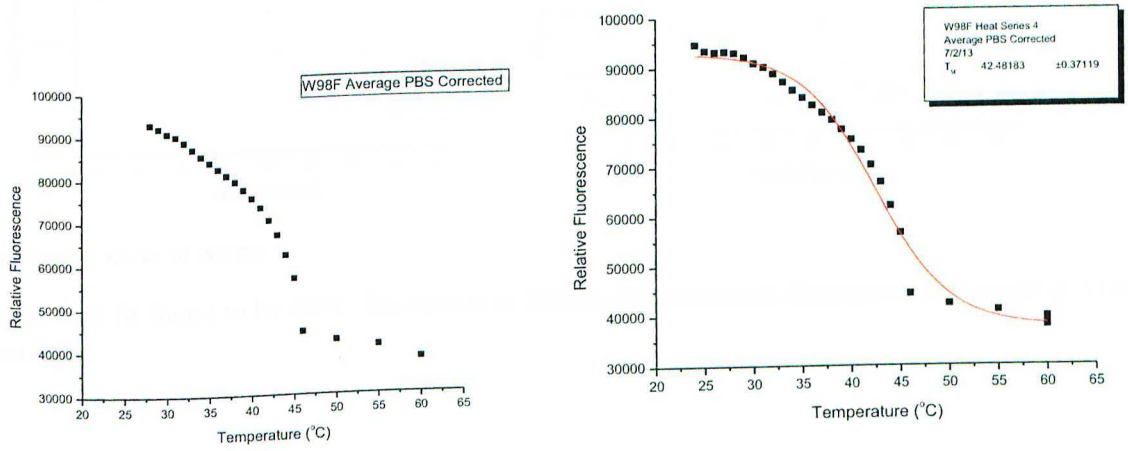

Figure 19. IF Curve of W98F

T_M by best fit found to be 42°C. Excitation at 280nm and maximum fluorescent emissions at 314nm were measured.

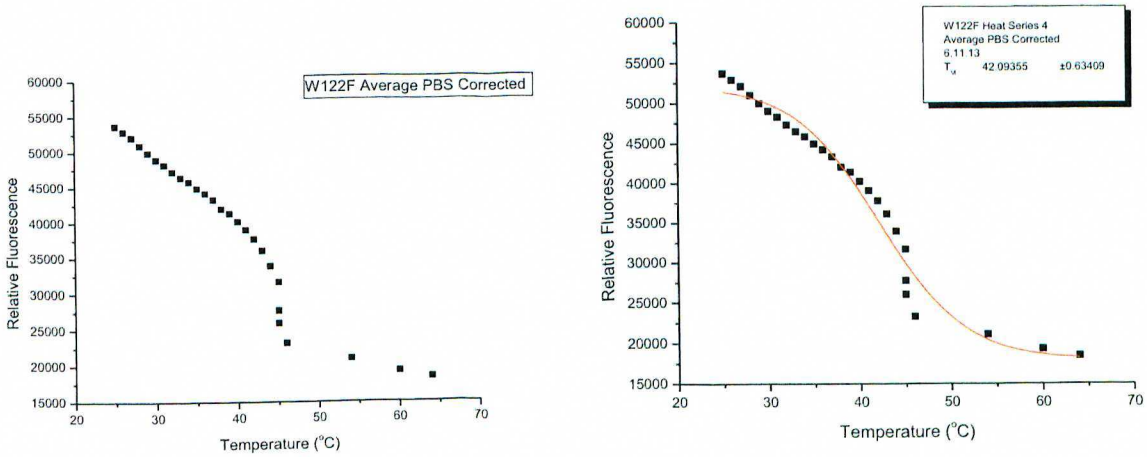

Figure 20. IF Curve of W122F

T_M by best fit found to be 42°C. Excitation at 280nm and maximum fluorescent emissions at 314nm were measured.

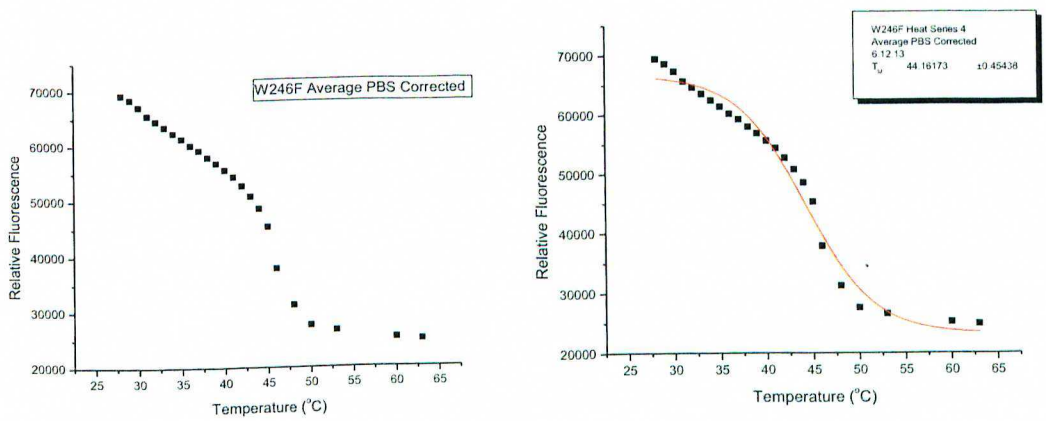

Figure 21. IF Curve of W246F

T_M by best fit found to be 44°C. Excitation at 280nm and maximum fluorescent emissions at 314nm were measured.

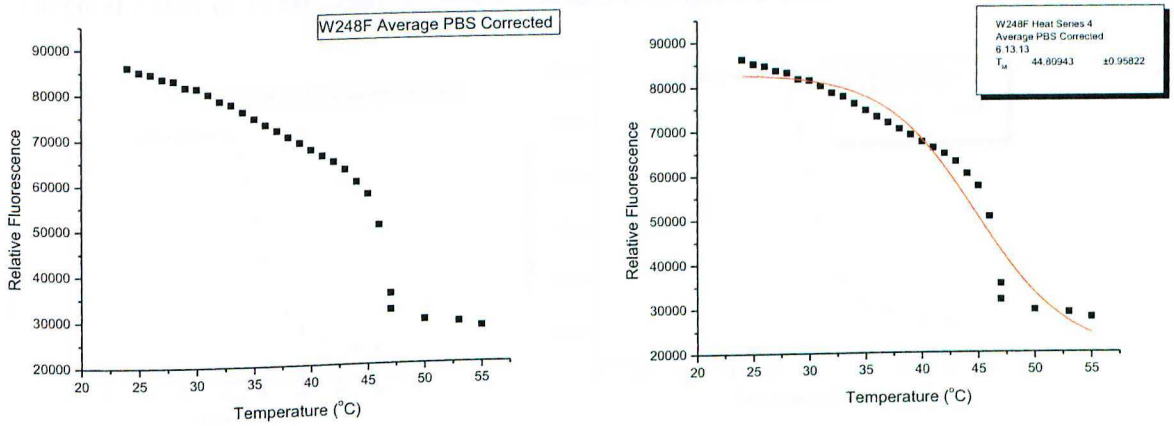

Figure 22. IF Curve of W248F

T_M by best fit found to be 44°C. Excitation at 280nm and maximum fluorescent emissions at 314nm were measured.

The variants W98F, W122F, W246F, and W248F were fit to a single sigmoidal curve; however, appears that there is a two stage process between folded and unfolded states (figures 19, 20, 21, 22). The second stage of denaturation is more clearly shown by a larger decrease in overall fluorescence. The T_M values generated by the best curve fit do not clearly describe the first or second midpoints of any of these curves. More suitable T_M values for the W122F curve are 34°C and 44°C (figure 20). The data representing variant W246F's denaturation appears to have two stages centered at 36°C and 47°C (figure 21). It is difficult to assign a more appropriate T_M value for the first denaturation stage of variant W248F's curve because it is very gradual (Figure 22). The second, more intense phase T_M value would be 47°C (Figure 22).

IF Thermal Assay of W246_248F Rv0045c Variant is Single Phased.

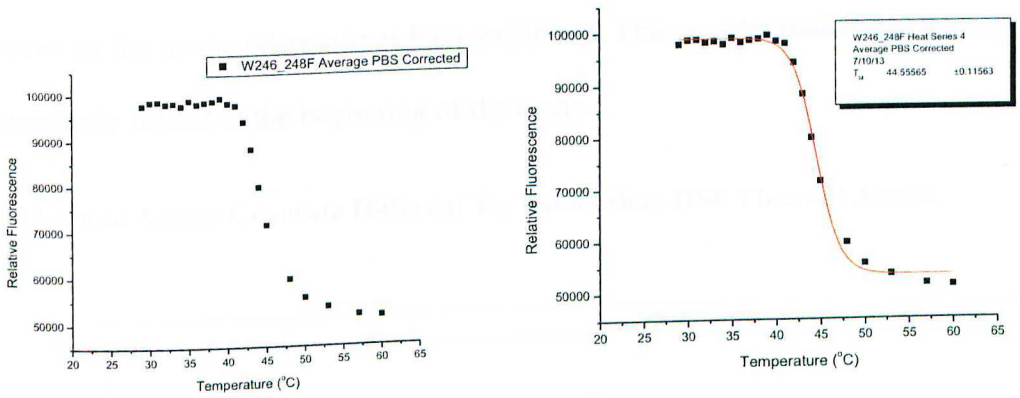

Figure 23. IF Curve of W246_248F

T_M by best fit found to be 44°C. Excitation at 280nm and maximum fluorescent emissions at 314nm were measured.

Variant W246_248F fit well to a single sigmoidal curve (figure 23). Unlike its parent variants W246F and W248F, W246_248F did not exhibit a biphasic like denaturation curve. The reported T_M by IF accurately describes the midpoint of the data.

IF Thermal Assay of W122_246F Rv0045c Variant is Potentially Biphasic.

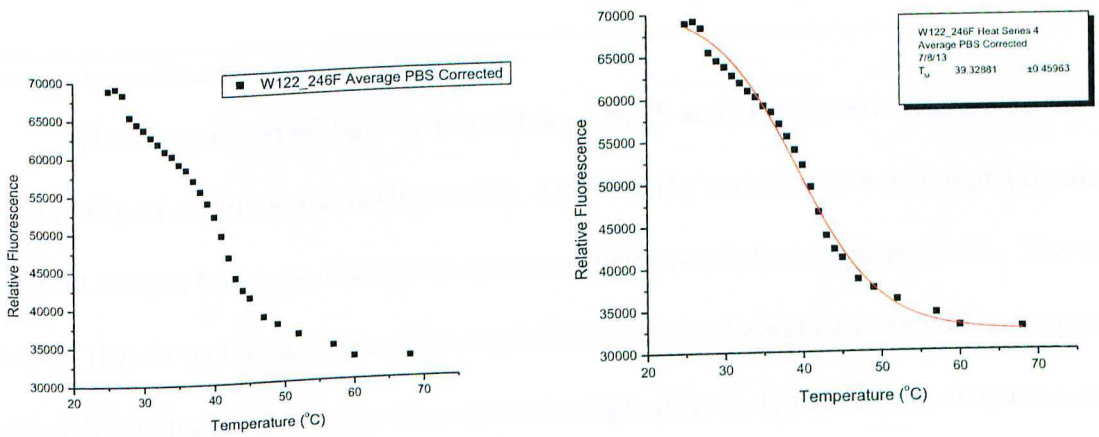

Figure 24. IF Curve of W122_246F

T_M by best fit found to be 39°C. Excitation at 280nm and maximum fluorescent emissions at 314nm were measured.

Variant W122_246F was fit to a single stage sigmoidal curve, which does not best describe its denaturation process (figure 24). Similar to its parent variants W122F and W246F,

W122_246F exhibits a possible biphasic denaturation curve. The far left most points in figure 24 are not as flat as the other curves have exhibited. This may be indicative of the protein not being completely folded at the beginning of the assay.

IF Thermal Assays Generate Different T_M Values than DSF Thermal Assays

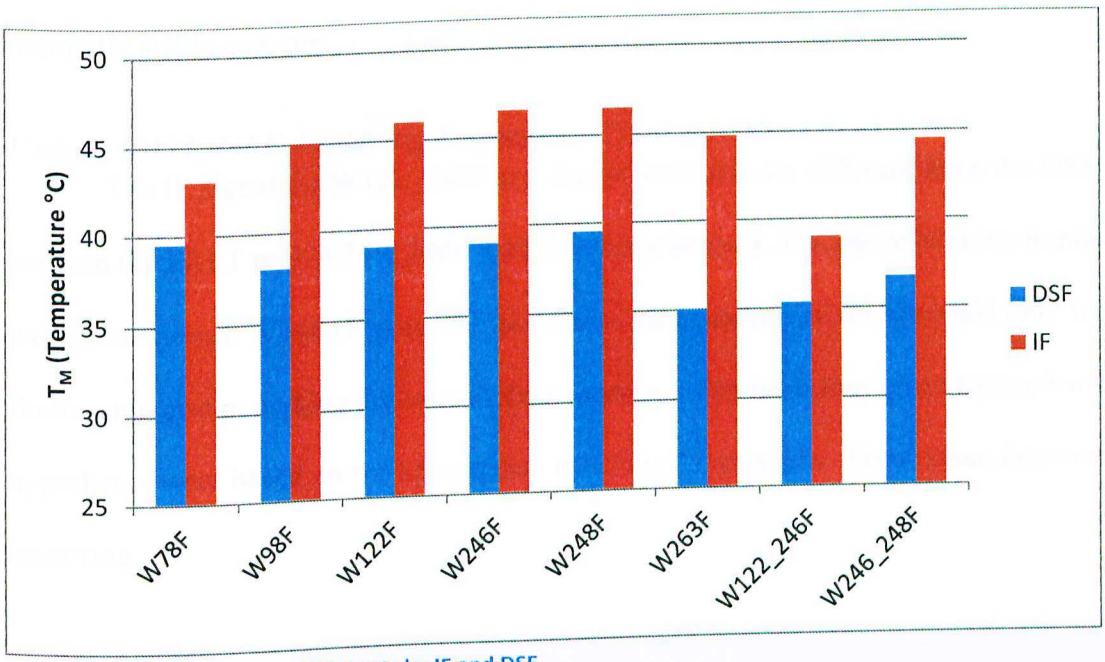

Figure 25. Thermal Stability of Mutants by IF and DSF

The comparison of T_M's values obtained by IF and DSF reveal different trends relating the stability of certain variants (figure 25). All Rv0045c variants have different T_M values by the different assays; however, there is no common difference between the methods. The two variants that fit well to a single phase sigmoidal IF curve theoretically should correspond better to the DSF melt curves because they are both single phased. However, this is not the case. W78F and W263F have two different T_M values from both methods, and the deviation between those methods is different as well. The difference between W78F's IF and DSF determined T_M values is 2.5°C; W263F's difference is nearly 10°C. Even acknowledging the associated error with DSF (+/- 1°C) and IF (+/- 2°C) the difference for W263F is significant. The fitting to a single phased

sigmoidal curve in the IF method does not necessarily correspond to the DSF determined T_M value, which supports that IF is monitoring a different unfolded state than DSF. DSF correlates to the hydrophobic pockets of a protein, while IF is monitoring the quenching interactions between fluorescent residues. Alone, neither IF or DSF provides the entire picture. The only common trend between the DSF and IF data series is that variant W122_246F was the least thermally stable enzyme.

Variant W122_246F displaying Tryptophan-Tyrosine Interactions.

The IF signal for W122_246F was hypothesized to be different from the DSF signal because the FRET pair W246_248F would be knocked out. The phenylalanine in place of W246 would not quench W248 (Figure 26). Similarly, the mutation at W122 would only remove a fluorescing group, making the overall fluorescence come from four other tryptophans. These hypotheses were based on the assumption that only Tryptophan- Tryptophan interactions were occurring.

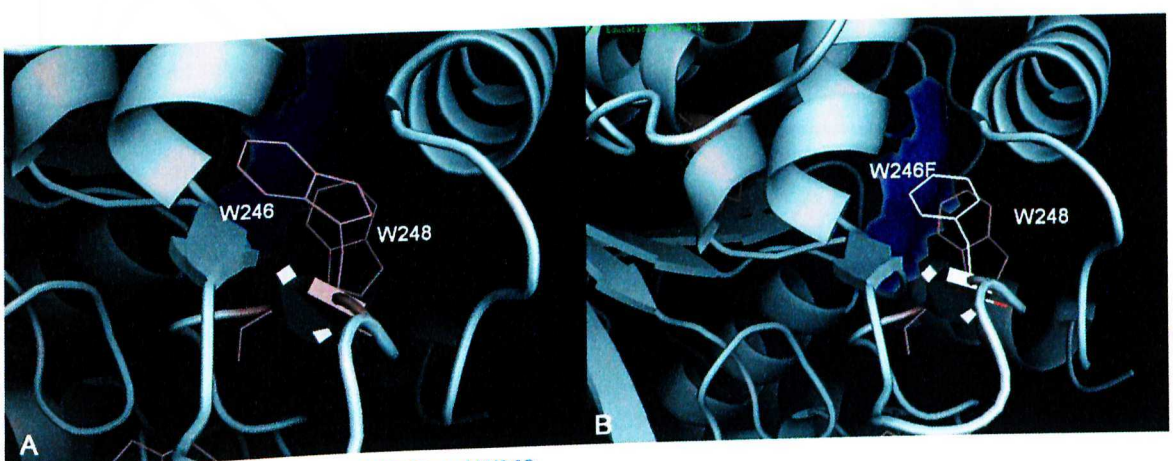

Figure 26. Rv0045c (cartoon) Close up of W246 and W248

Cartoon depiction of Rv0045c, active site shown in blue, tryptophans in violet. **A.** both tryptophans are shown. **B.** W246 has been mutated to W246F.

Tryptophan-Tryptophan interactions are possible; however, the emissions recorded were not in the expected range (Appendix E). The observed emission, 314nm, is almost consistent

with the reported blue shift (wavelength less than 340nm) observed when tryptophans are in a hydrophobic environment[7]; however 314nm is much lower than the experimentally observed blue shift around 325nm.

Based on this data, the assumption that tryptophan fluorescence was being monitored is potentially incorrect and instead another fluorescent moiety of Rv0045c is being observed. Tyrosine has a similar range of absorption and emission wavelengths and is capable of FRET (figures 27 and 28). However, 314nm is not indicative of any of the perfect Trp-Trp or Tyr-Trp scenarios. Tryptophan exciting tyrosine in a FRET phenomenon would have a resultant fluorescence around 310nm, much closer to the experimentally observed 314nm (Figure 27). There are two tyrosines in Rv0045c that are in close proximity with tryptophans: Y250 and Y128.

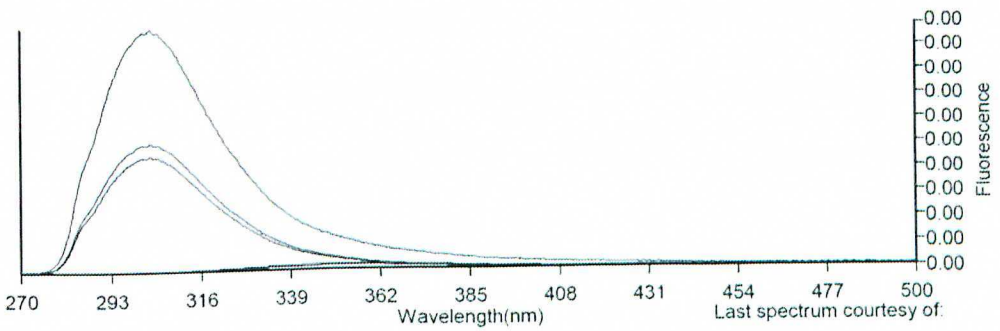

Figure 27. Simulated FRET, Trp exciting Tyr

The resulting fluorescence is the top curve in the graph, peaking around 310nm [17, 18].

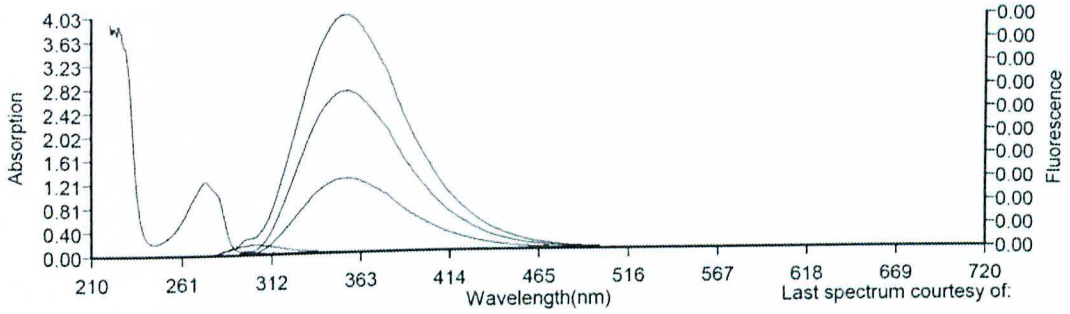

Figure 28. Simulated FRET, Tyr exciting Trp

This graph shows a tyrosine residue's emission exciting a tryptophan; the resulting fluorescence is shown by the top curve peaking around 360nm [17, 18].

The W122_246F was meant to knock out the W246 W248 pair and this was successful; however, according to the crystal structure W248 is also likely to be interacting with Y250 (figure 29), which is only 4.6 angstroms apart, and is still quenched by a different partner. A tyrosine-tryptophan pair was also eliminated in W122_246F accidently (panel C). W122 is near Y128, only 5.6 angstroms apart (figure 29). In the W122_246F mutant, this trp-tyr relationship was eliminated as can be seen in panel D.

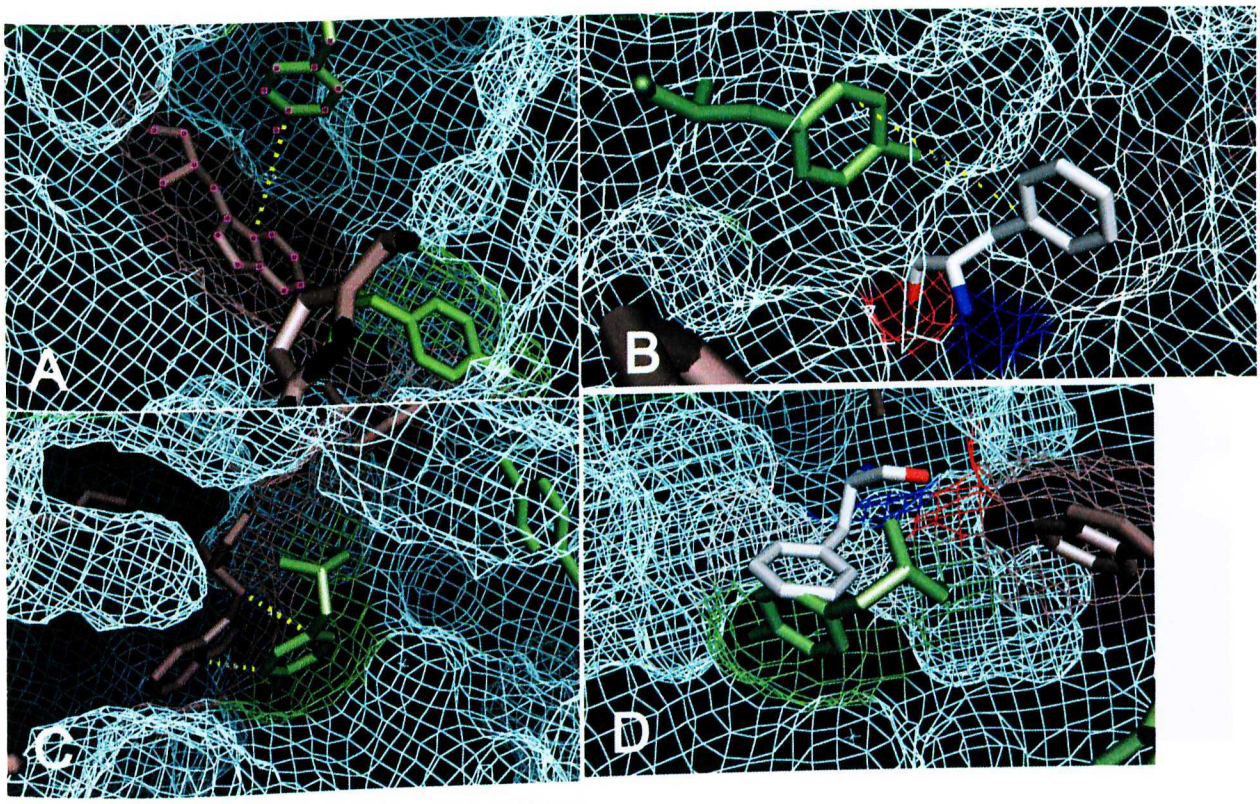

Figure 29. Rv0045c (mesh) Close up of Tyrosine and Tryptophan Pairs

Tyrosines are depicted in green, tryptophans in violet, and (mutated) phenylalanine residues in white. **A.** Close up of W122 and Y128. Measured to be 5.6 Å apart. **B**. Close up of W122F and Y128. **C**. Close up of W248 and Y250. Measured to be 4.6 Å apart. **D**. Close up of W246F, W248 and Y250.

The goal of using intrinsic fluorescence to create a simple description of the denaturation pathway of Rv0045c was not completely thwarted, but derailed, by the realization of these interactions with tyrosine. Fluorescence may not provide a simple, clear picture of the unfolding; however, the target mutations can still be evaluated to determine the future viability of this method.

Conclusion

Overall the mutagenesis, transformation, and purification of these desired enzymes were nearly successful. Intrinsic fluorescence, as a methodology, was vetted by these experiments and proven possible with Rv0045c. The actual desired enzyme, a quadruple mutant was out of reach

and unfeasible with the current experimental design. The loss of catalytic activity in W246_248_263F prevents further mutagenesis into the quadruple mutant W122_246_248_263F (figure 30). Without enzymatic activity, the possibility of using the quadruple mutant as a model for the denaturation of Rv0045c is significantly lessened. Any further work utilizing this methodology requires a different approach to manipulating the fluorescent amino acid residues.

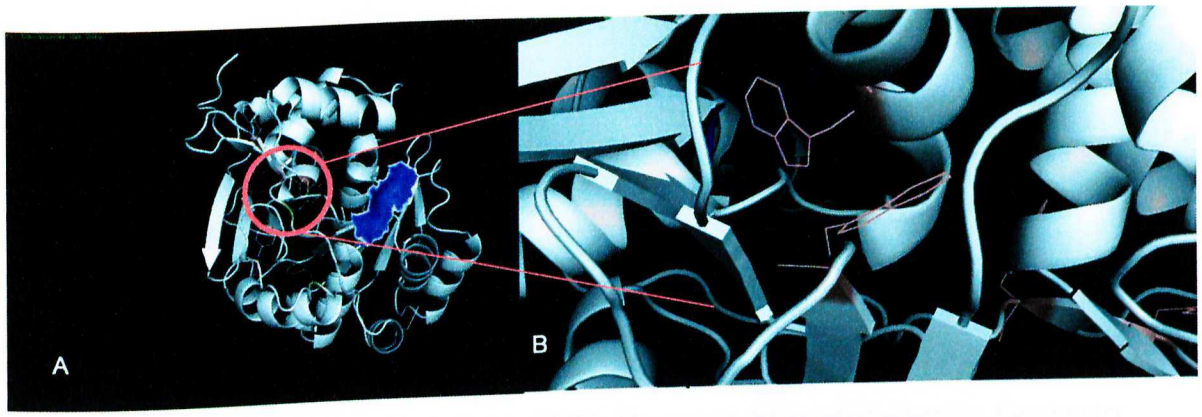

Figure 30. Proposed quadruple Rv0045c variant (cartoon)

Cartoon depiction of Rv0045c, active site shown in blue, tryptophans in violet. A. Proposed quadruple mutant W122_246_248_263F. B. Close up of FRET pair W78 and W98F in proposed quadruple mutant.

Future Work

One remaining question concerning the IF thermal assay is: why were all of the emissions at 314 nm? To determine whether it was in fact tyrosine-tryptophan interactions of the blue shift of tryptophans, mutagenesis of tyrosine should be considered. If one of the tyrosines was to be mutated to phenylalanine and the intrinsic fluorescence assay repeated, it could explain the emission wavelength. If truly tyrosine-tryptophan interactions are occurring, the wavelength of the emission would no longer be 314nm. If the resultant emission is still 314nm, it indicates that the tryptophan's fluorescence emission is being shifted by its environment.

References

1. Cole ST, Brosch R, Parkhill J (1998) Deciphering the biology of *Mycobacterium tuberculosis* from the complete genome sequence. *Nature* 393: 537-4

2. Jiubiao G, Xiangdong Z, Lipeng X, Zhongyuan L , Kehui X, Shentao L, Tingyi W, Siguo L, Hai P (2010). Characterization of a Novel Esterase Rv0045c from *Mycobacterium tuberculosis*. *PLoS One* 5.10

3. Xiangdong Z, Jiubiao G, Lipeng X, Honglei , Dongwei Z, Kai Z, Fei S, Tingyi W, Siguo L, Hai P. (2011). Crystal Structure of a Novel Esterase Rv0045c from *Mycobacterium tuberculosis*. *PLoS One* 6.5

4. Lehninger A., Nelson D.N., & Cox M.M. (2008) *Lehninger Principles of Biochemistry*. W. H. Freeman, fifth edition.

5. Niesen, F.H., Berflund, H., and Vedadi, M. (2007) The use of differential scanning fluorimetry to detect ligand interactions that promote protein stability, *Nat Protoc* 2, 2212-2221.

6. Lavis, L.D., and Raines, R.T. (2008). Bright ideas for chemical biology. *ACS Chemical Biology*, 3 (3), DOI: 10.1021/cb700248m. Date Accessed 15 April 2013.

7. Raman, R., Prak, C.P., Hsieh, C., Oswald, R.E., Chang, Y., and Y. Sharma. (2013). The perturbation of tryptophan fluorescence by phenylalanine to alanine mutations identifies the hydrophobic core in a subset of bacterial Ig-like domains. *Biochemistry*; 52, 4589-4591.

8. Raha, P., Chattopadhyay, S., Mukherjee, S., Chattopadhyay, R., Roy, K., and S. Roy. (2010). Alternative Sigma Factors in the Free State are Equilibrium Mixtures of Open and Compact Conformations. *Biochemistry*, Issue 49. DOI: 10.1021/bi1011173. Date Accessed 3 January 2014.

9. Pierce, B.D., Toptygin, D., and B. Wendland. (2013). Pan1 is an intrinsically disordered protein with homotypic interactions. *Proteins*;81: 1944-1963.

10. Engel, T and W. Hehre. Quantum Chemistry and Spectroscopy (3rd ed). Boston: Pearson.

11. Lavis, L.D., Chao, T. and Raines, R.T. (2011). Synthesis and utility of fluorogenic

acetoxymethyl ethers. *Chemical Science*, Issue 3. DOI: 10.1039/c0sc00466a Date Accessed 15 April 2013.

12. QuikChange II site-directed mutagenesis kit instruction manual. Agilent Technologies Inc., Santa Clara,CA. Accessed Jan 31st 2013, http://www.genomics.agilent.com/files/Manual/200523.pdf

13. Ausubel, FM, R Brent, RE Kingston, DD Moore, JG Seidman, JA Smith, & K Struhl (1999). "*Escherichia coli*, plasmids, and bacteriophages." *Short Protocols in Molecular Biology*. 4th edition. New York: John Wiley & Sons. p1.1-1.12

14. High-Speed Plasmid Mini Kit Instruction Manual. IBI Scientific, Peosta, IA. Accessed Feb 7th 2013. http://www.ibisci.com/images/ IB47100IB47101IB47102Protocol.pdf

15. *The QIAexpressionist*. (2003). "A handbook for high- level expression and purification of 6xHis-tagged proteins." Qiagen, Valencia CA. fifth edition.

16. BL21-Codon Plus Competent Cells Instruction Manual. Agilent Technologies Inc, Santa Clara, CA. Accessed March 15th 2013. http://www.genomics.aagilent.com/files/manual/230240.pdf

17. Du, H. Fuh, R., Li, J, Corkan, L.A., Lindsey, J.S. (1998). "PhotochemCAD. A computer-aided design and research tool in photochemistry and photobiology." *Photochem. Photobiol.* 68, 141-142.

18. Dixon, J.M. Taniguchi M., Lindsey, J.S. (2005). "PhotochemCAD2. A refined protein with accompanying spectral databases for photochemical calculations." Photochem. Photobiol. 81, 212-213.

APPENDICES

Appendix A: PCR gels

Supplemental Figure 1.1 W78F and W263F PCR gel: Lane 1: MW marker. Lane 2: W78F one. Lane 3: W78F two. Lane 5: W263F one. Lane 6: W263F two. Lane 7: negative control. Lane 8: positive control. Note* Bacterial transformation was performed using the digested PCR products of lane 2 and 5.

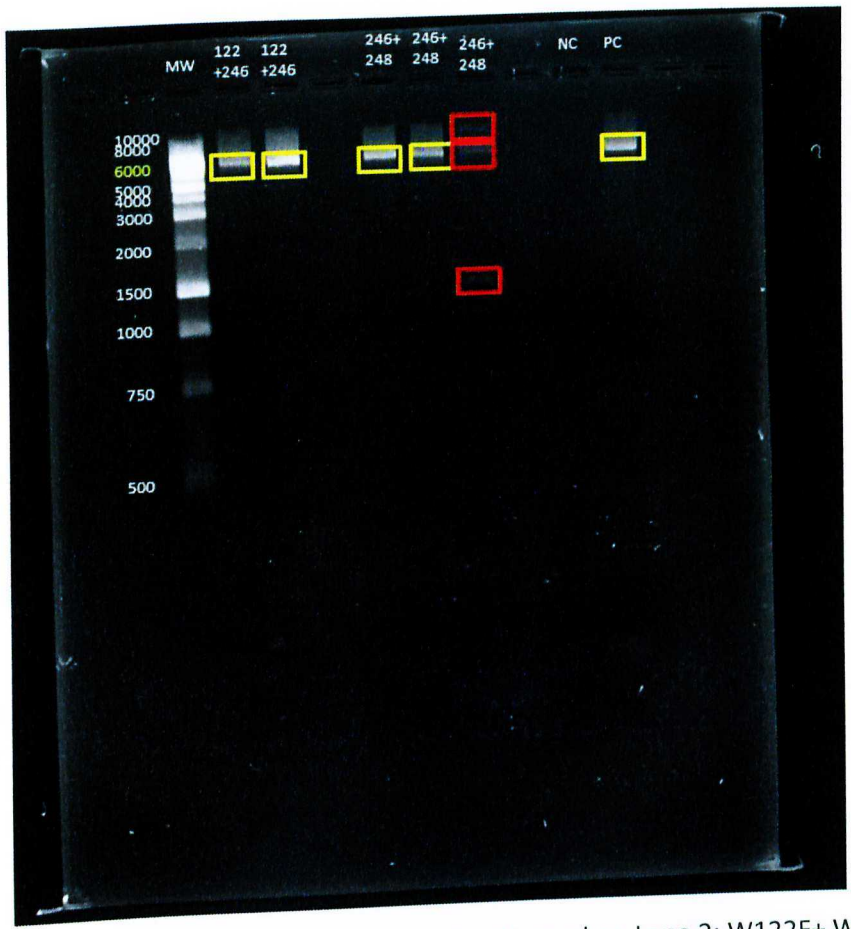

Supplemental Figure 1.2. Double Mutants PCR. Lane 1: MW marker. Lane 2: W122F+ W246F. Lane 3: W122F + W246F. Lane 5: W246F+ W248F. Lane 6: W246+ W248F.Lane 7: W246F + W248F. Lane 9: negative control. Lane 10: Positive control. The Agarose gel was run in TBE buffer at 100V for 45 minutes.
Note* Lane 7 has extra bands of unreacted oligos (I think) so it was thrown out.
Note** Bacterial transformation was performed with the digested PCR products of lane 2 and lane 5.

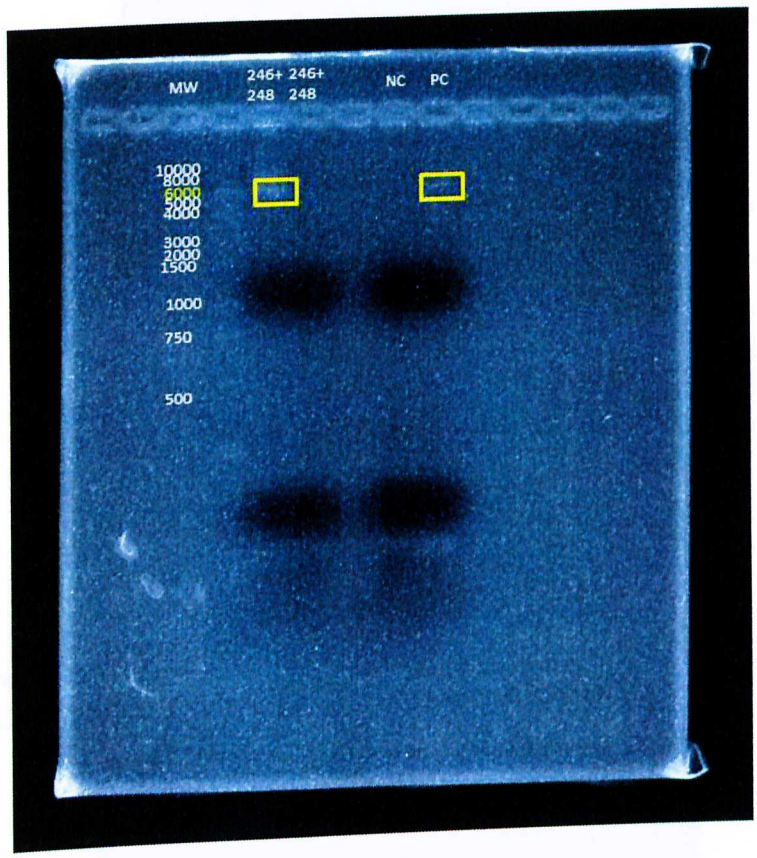

Supplemental Figure 1.3 W246_248F PCR: Lane 1: MW marker. Lane 2: W246F+W248F A. Lane 3: W246F+W248F. Lane 5: Negative Control. Lane 6: Positive Control.
Note* Bacterial transformation was performed using the digested PCR products from lane 2.

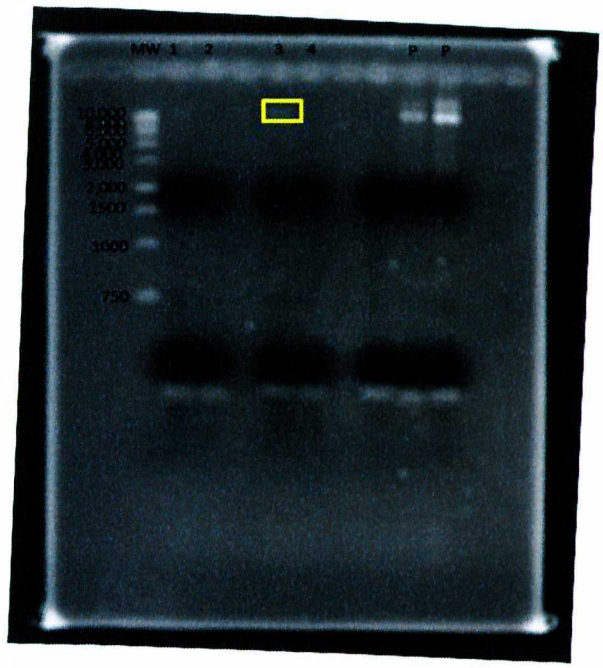

Supplemental Figure 1.4 W78_263F and W246_263F PCR gel l: Lane 1: W78_246F A. Lane 2: W78_246F B. Lane 3: W246_263F A. Lane 4: W246_263F B. Ran for 45 minutes at 100V.

Supplemental Figure 1.5 W246_248 PCR Gel. Lane A= W246_248F 1.Lane B= W78_246F 2. Lane C= W78_246F 3. Run at 100V for 45 minutes.

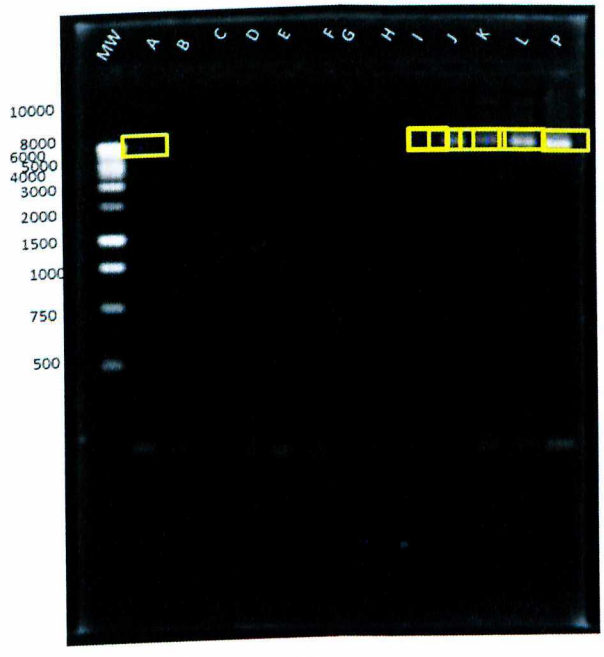

Supplemental Figure 1.6 Triples PCR Gel. Lane 1: MW marker. A= W246_248F 1. B= W246_248F 2. C=W122_246_248F 1. D= W122_246_248F 2. E= W122_246_263F 1. F=W122_246_263F 2. G= W78_246_248F 1. H= W78_246_248F 2. I= W122_246_263F 1. J= W122_246_263F 2. K=W246_248_263F 1. L= W246_248_263F 2. The gel was run in TBE buffer at 100x for 45 minutes.

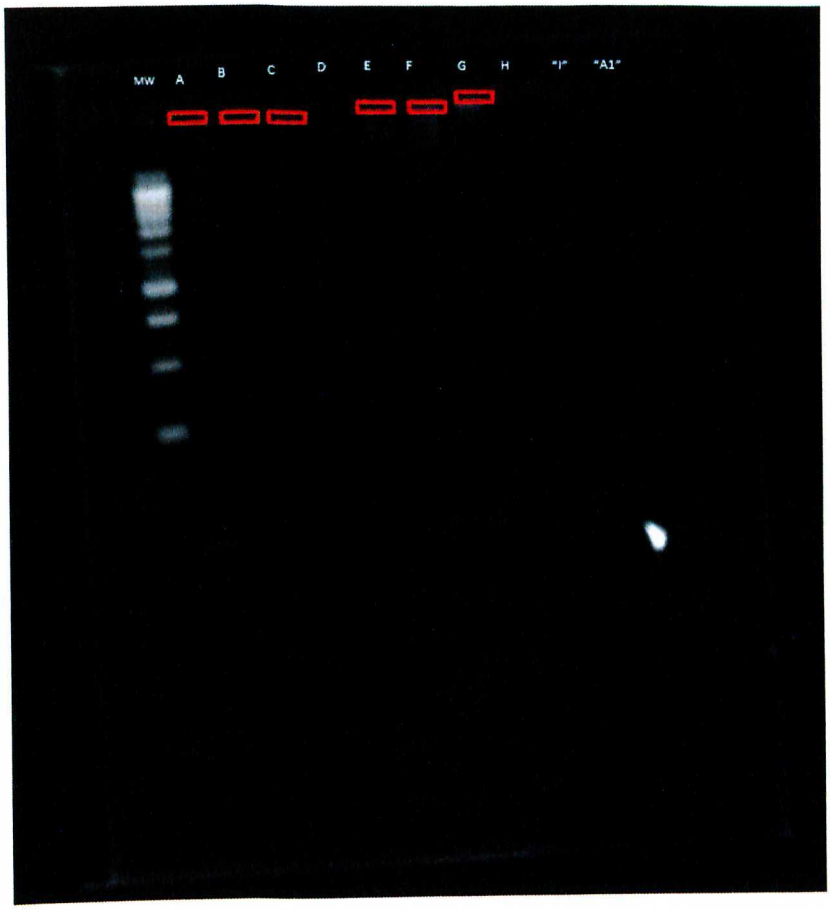

Supplemental Figure 1.7 Double PCR gel. Lane 1: MW marker. Lane 2: A (W78_122F). Lane 3: B (W78_263F). Lane 4:C (W122_78F). Lane 5: D (W122_263F) .Lane 6: E(W246_78F). Lane7: F(W248_78F). Lane 8: G(W248_122F). Lane 9: H(W248_263F). Lane 10: "I"(W122_246_263). Lane 11: "A1" (W78_246F). The 1.5% agarose gel was run in 1X TBE buffer at 120V until completion. It was visualized in EtBr.

Appendix B: SDS PAGE

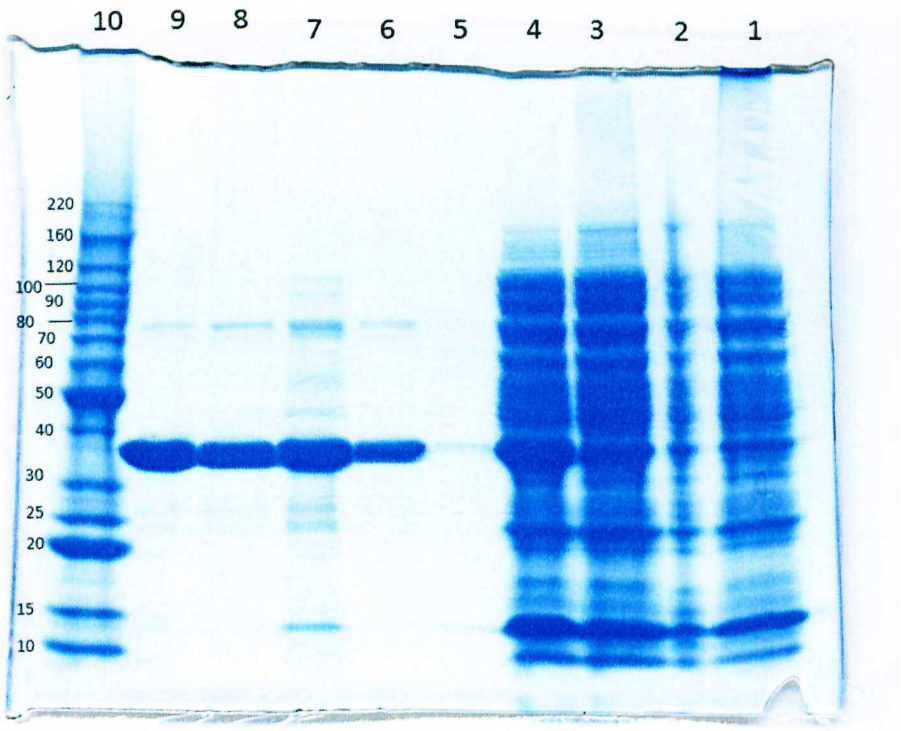

Supplemental Figure 2.1 SDS PAGE Analysis of single Rv0045c Mutants. Lane 1: W98F flowthrough. Lane 2: W122F flowthrough. Lane 3: W246F flowthrough. Lane 4: W248F flowthrough. Lane 5: W122F second wash. Lane 6: W98F pure. Lane 7: W122F pure. Lane 8: W246F pure. Lane 9: W248F pure. Lane 10: Benchmark Protein Ladder. The 4-20% Agarose gel was run at 150V for two hours in 1X Tris Glycine buffer. It was visualized using SimplyBlue.

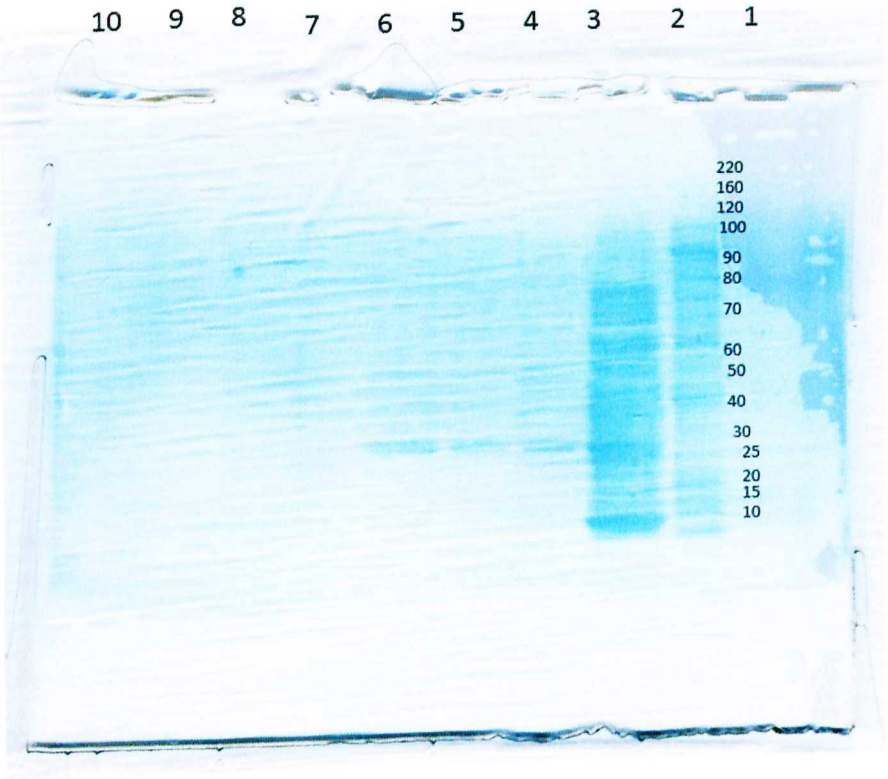

Supplemental Figure 2.2 W122_246F SDS PAGE. Lane 1: MW marker. Lane 2: Crude W122_W246F. Lane 3: Wash one. Lane 4: Wash two. Lane 5: Wash three.

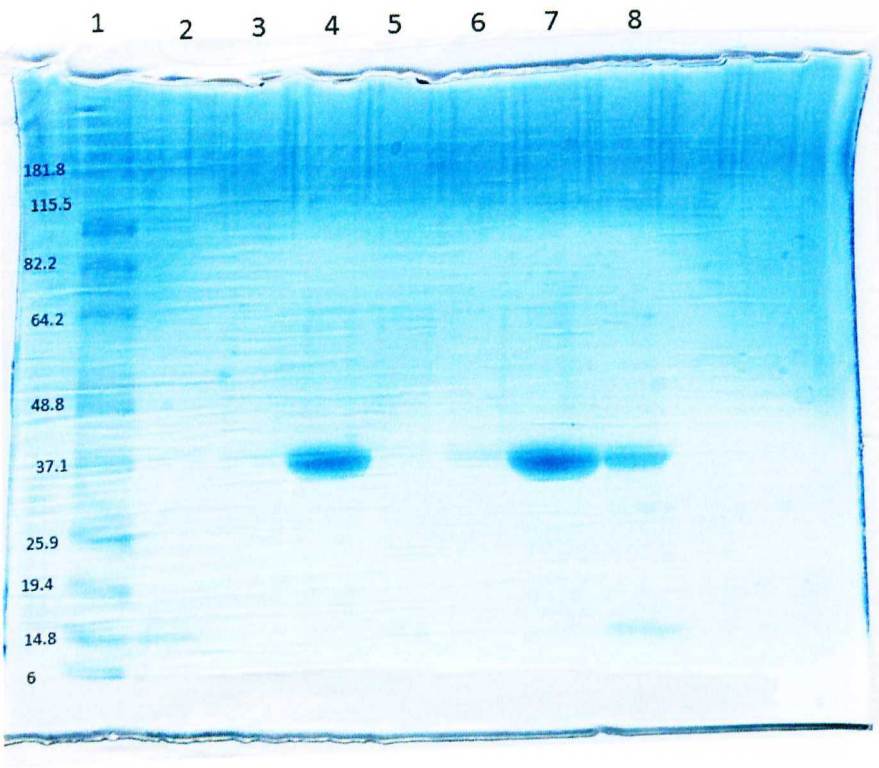

Supplemental Figure 2.3 W78F, W263F, and W122_246F SDS PAGE: Lane 1: MW marker. Lane 2: Wash one of W78F. Lane 3: Wash three of W78F. Lane 4: Pure W78F. Lane 5: Wash one of W263F. Lane 6: wash three of W263F. Lane 7: Pure W263F. Lane 8: Pure W122_W246F.

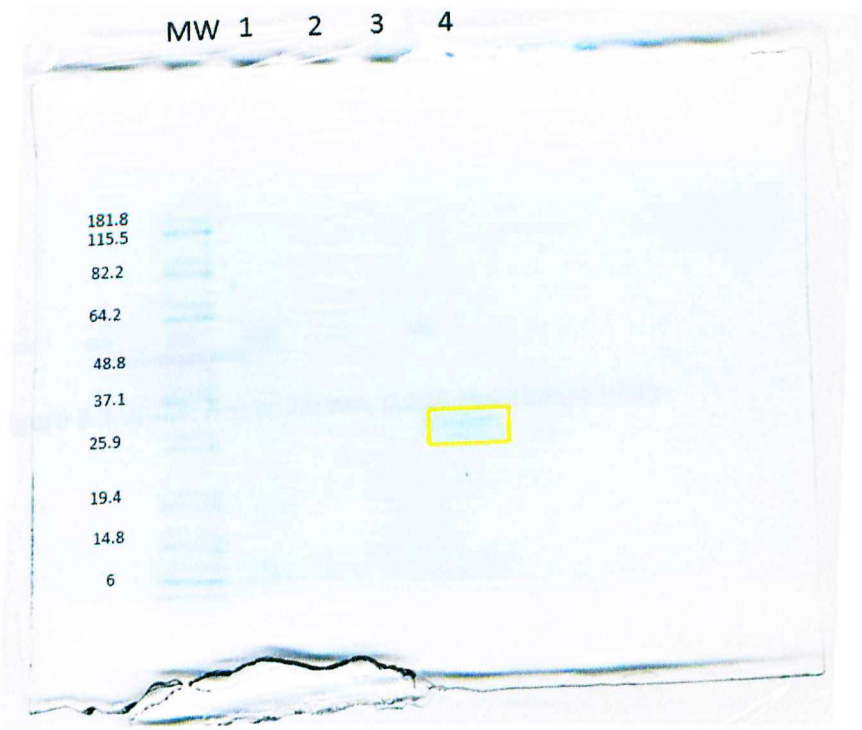

Supplemental Figure 2.4 W246_248F SDSPAGE MW marker, Simple Blue. Lane 1: Crude sample W246_248F. Lane 2: Was one sample W246_248F. Lane 3: Wash three sample W246_248F. Lane 4: pure W246_248F sample. 4-20% Tris Glycine gel run in tris glycine buffer at 150V for two hours.

Appendix C: Plasmid DNA Absorbance Spectra

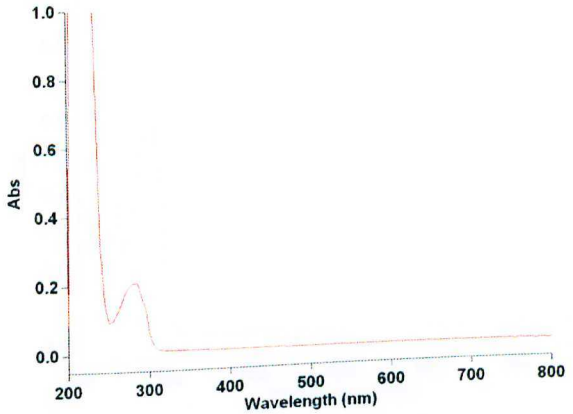

Supplemental Figure 3.1 W98F: Abs at 280nm, 0.205 absorbance units

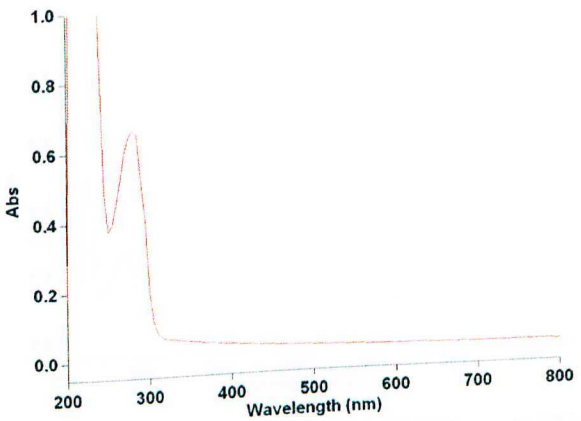

Supplemental Figure 3.2 W122F: Abs at 280nm, 0.662 absorbance units

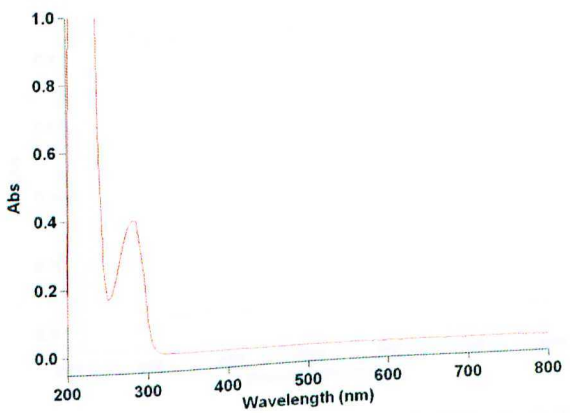

Supplemental Figure 3.3 W246F: Absat 280m, 0.396 absorbance units

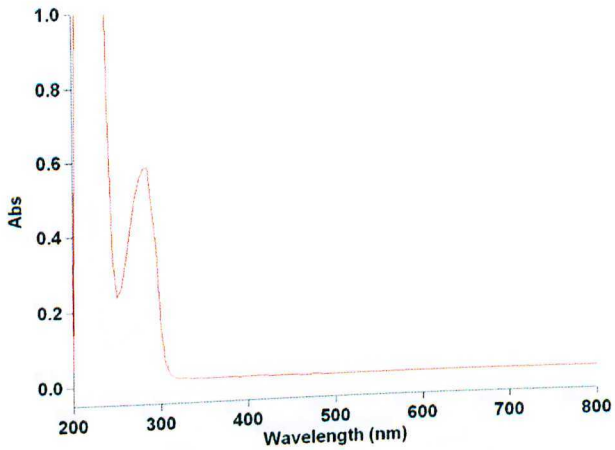

Supplemental Figure 3.4 W248F: Abs 280nm, 0.581 absorbance units

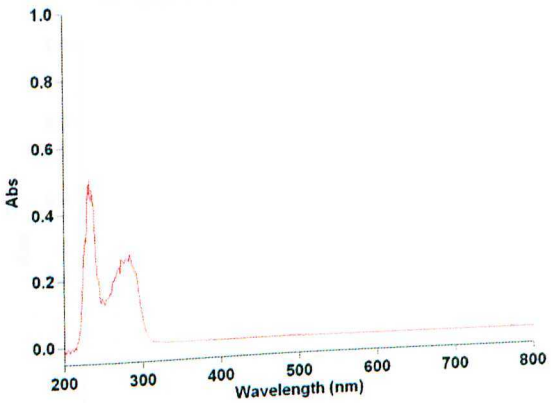

Supplemental Figure 3.5 W78F. Abs @ 280nm, 0.275 absorbance units

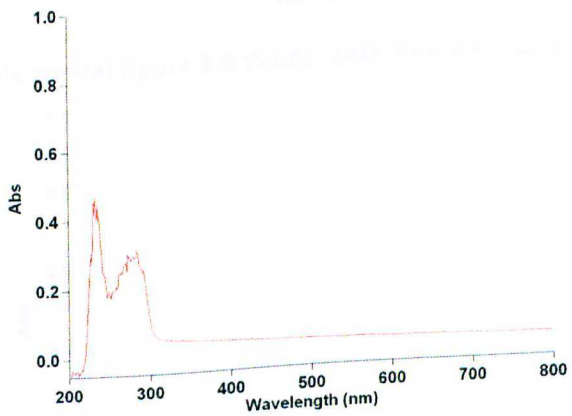

Supplemental Figure 3.6 W263F. Abs @ 280nm, 0.303 absorbance units

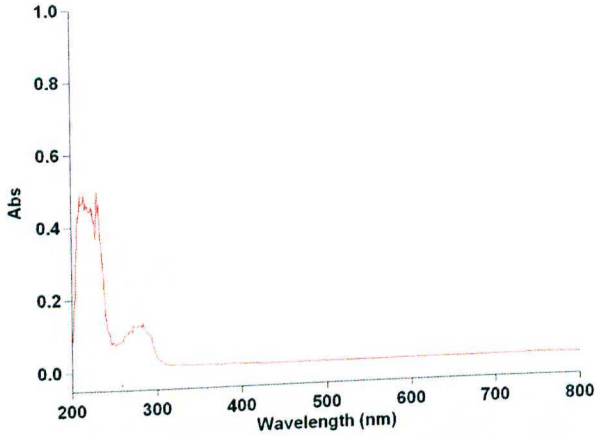

Supplemental figure 3.7 W122_246F Sample 1: Abs @ 280nm = 0.13 absorbance units

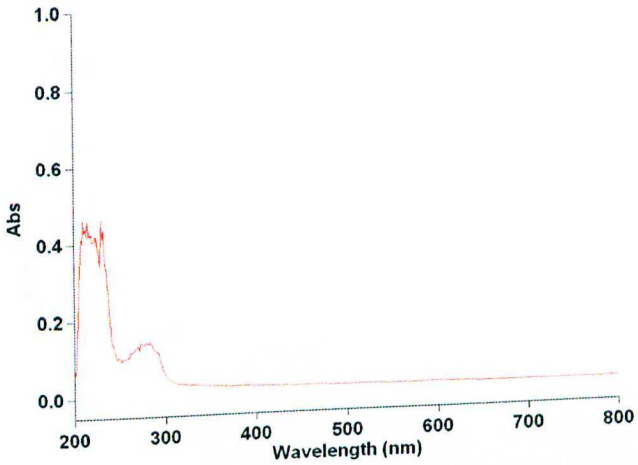

Supplemental figure 3.8 W122_246F Sample 2: Abs @ 280nm = 0.146 absorbance units

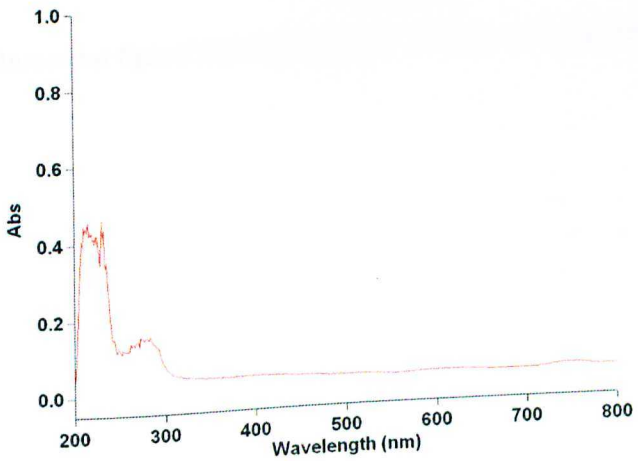

Supplemental figure 3.9 W122_W246F Sample 3: Abs @ 280nm = 0.153 absorbance units

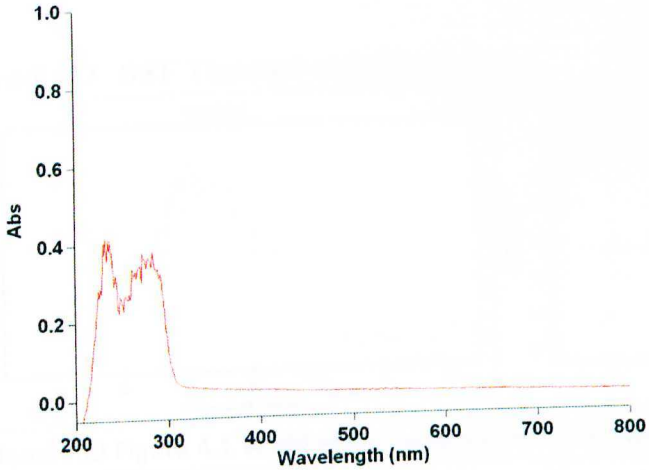

Supplemental figure 3.10 W246_248F sample 1 Abs @ 280nm = 0.362 absorbance units

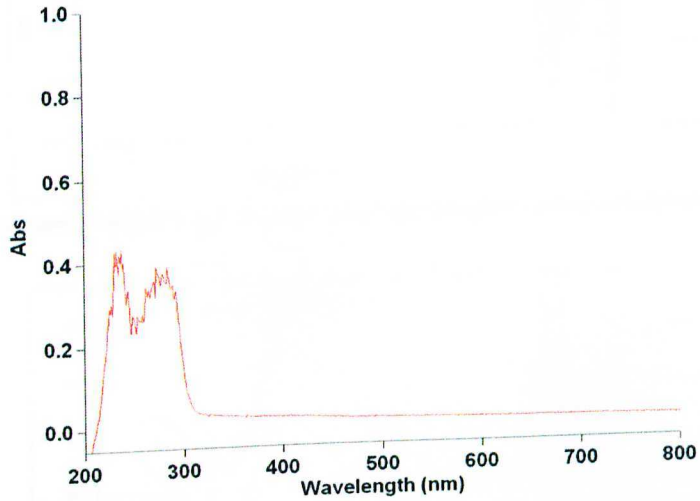

Supplemental figure 3.11 W246_248F Sample 2 Abs @ 280nm = 0.373 absorbance units

Appendix D: DSF Thermal stability assays

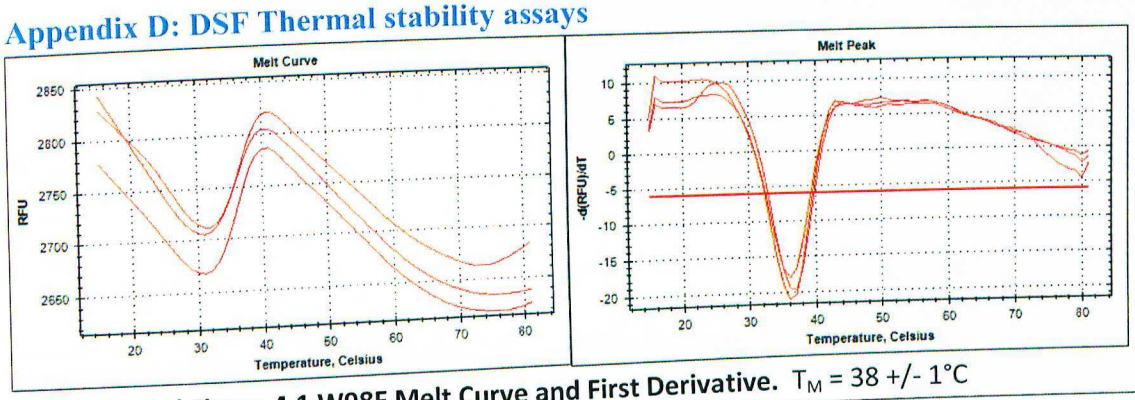

Supplemental Figure 4.1 W98F Melt Curve and First Derivative. T_M = 38 +/- 1°C

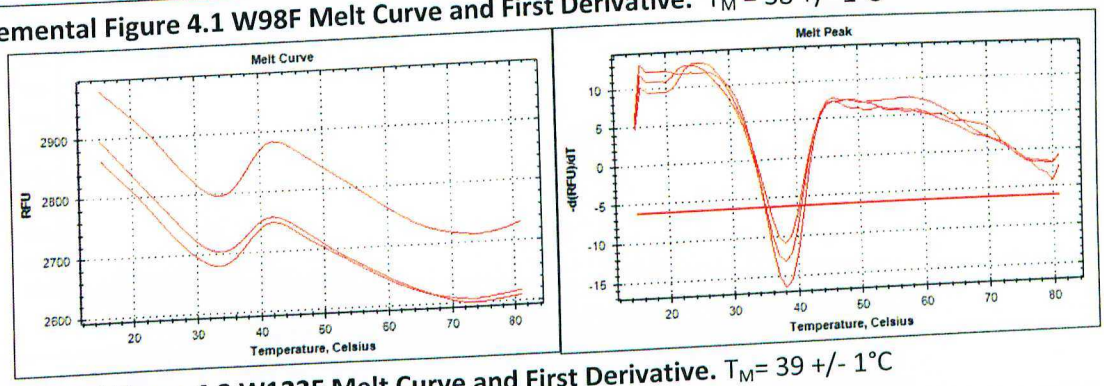

Supplemental Figure 4.2 W122F Melt Curve and First Derivative. T_M= 39 +/- 1°C

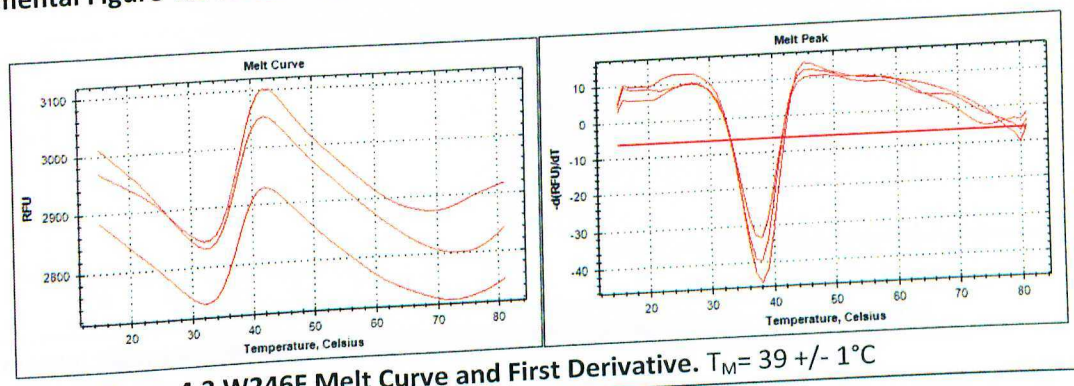

Supplemental Figure 4.3 W246F Melt Curve and First Derivative. T_M= 39 +/- 1°C

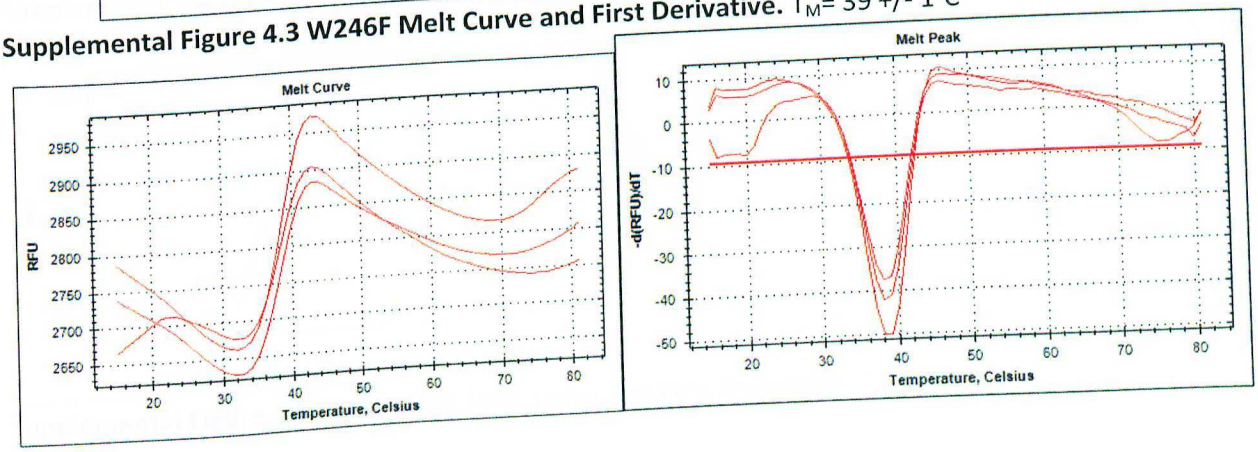

Supplemental Figure 4.4 W248F Melt Curve and First Derivative. T_M= 39.5 +/- 1°C

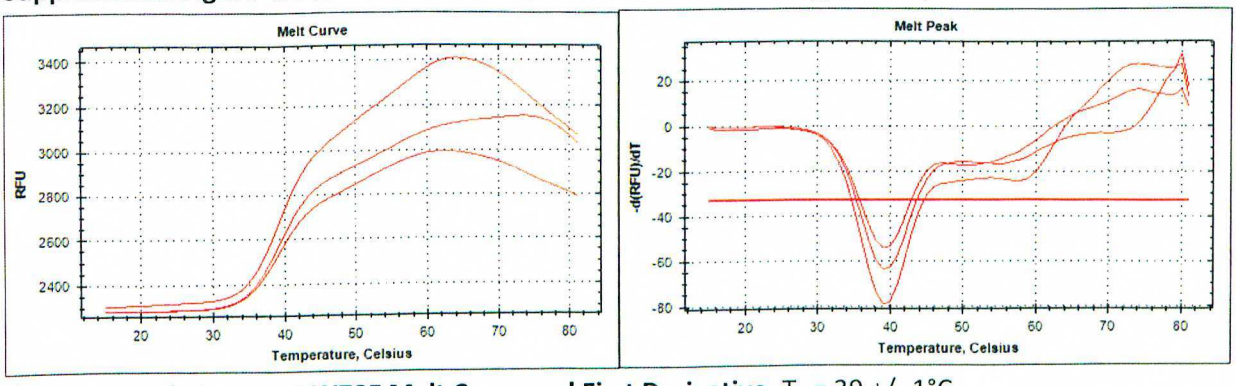

Supplemental Figure 4.5 W78F Melt Curve and First Derivative. T_M= 39 +/- 1°C

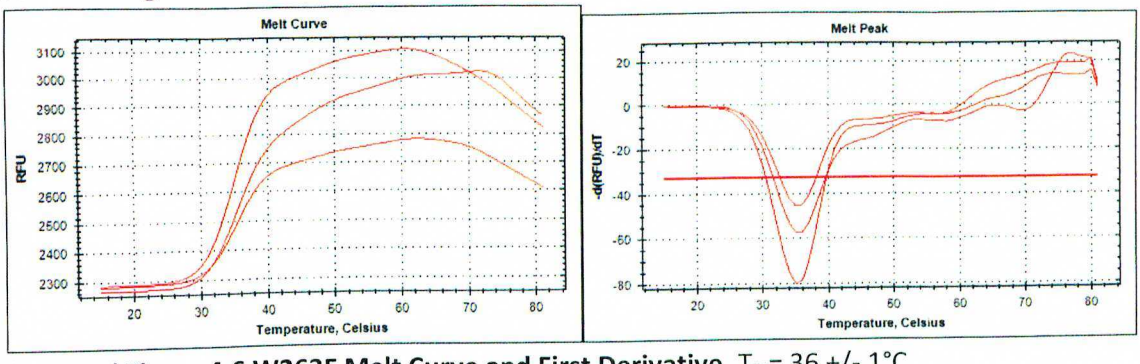

Supplemental Figure 4.6 W263F Melt Curve and First Derivative. T_M= 36 +/- 1°C

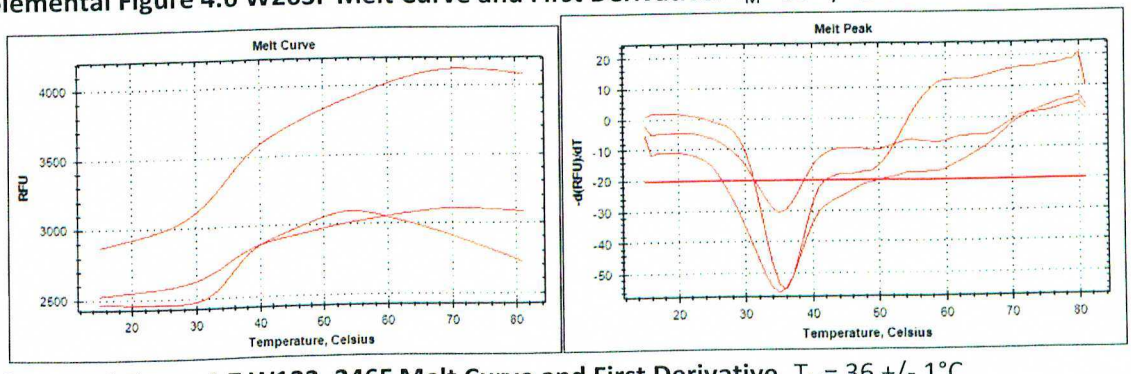

Supplemental Figure 4.7 W122_246F Melt Curve and First Derivative. T_M= 36 +/- 1°C

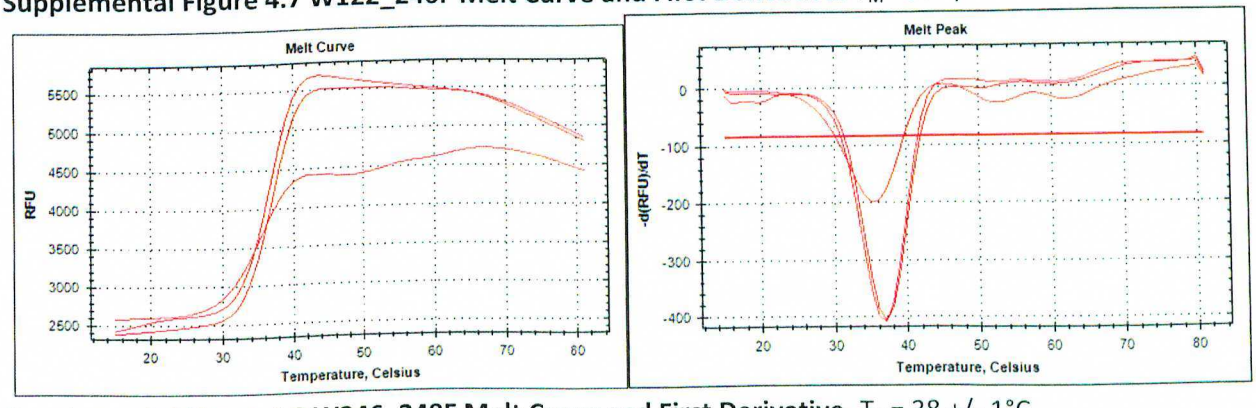

Supplemental Figure 4.8 W246_248F Melt Curve and First Derivative. T_M= 38 +/- 1°C

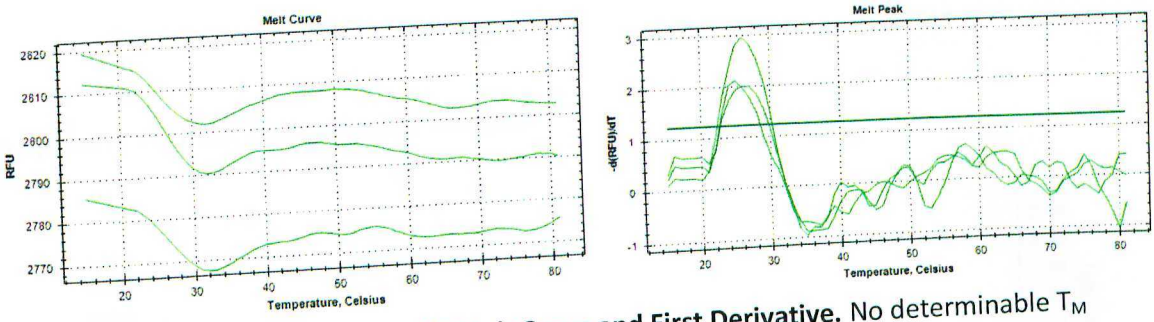

Supplemental Figure 4.9 W246_263F Melt Curve and First Derivative. No determinable T_M

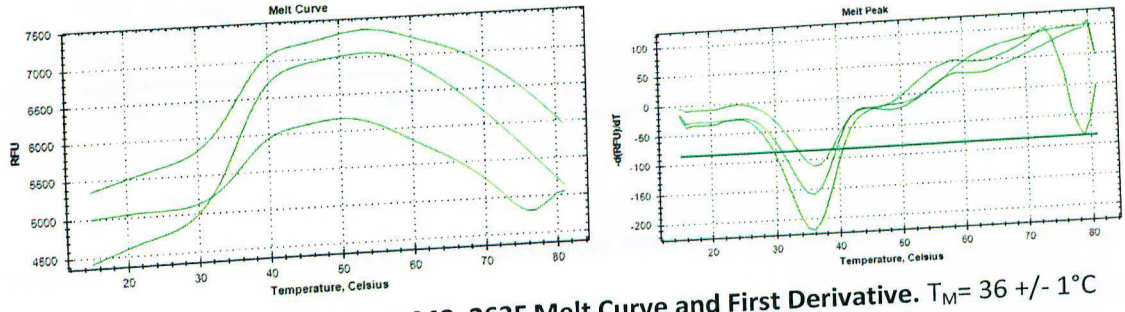

Supplemental Figure 4.10 W246_248_263F Melt Curve and First Derivative. T_M= 36 +/- 1°C

Appendix E: FRET Simulation Graphs

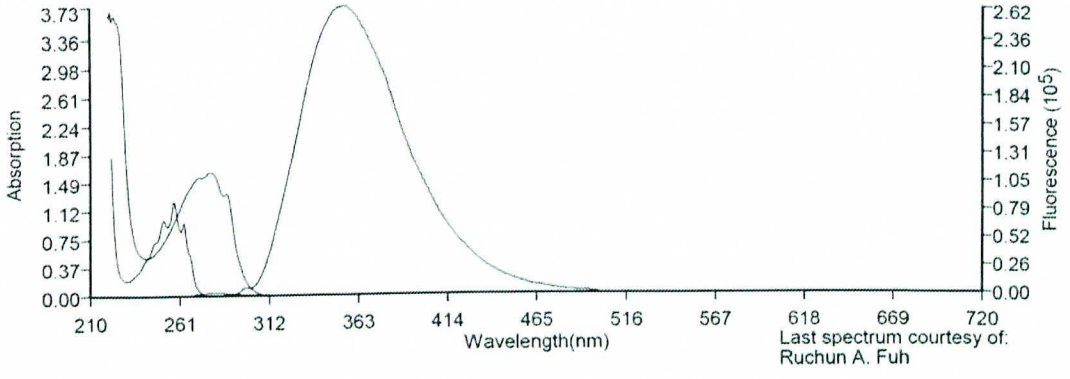

Supplemental Figure 5.1 Chart of the absorbance/ emissions of tryptophan and absorbance/ emissions of phenylalanine. The program PhotoChemCad2.1 could not perform a simulated FRET interaction between the two residues, regardless of proximity, angle, and other parameters.

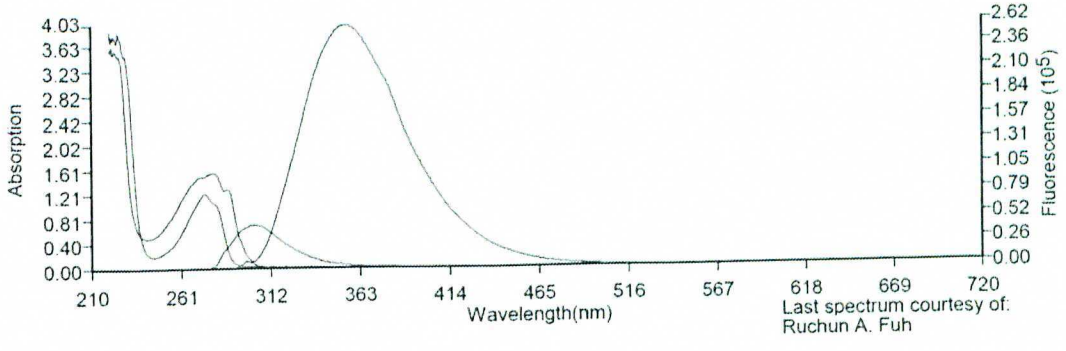

Supplemental Figure 5.2 Chart of the absorbance/ emissions of tryptophan and absorbance/ emissions of tyrosine. The program PhotoChemCad2.1 could not perform a simulated FRET interaction between the two residues, regardless of proximity, angle, and other parameters.

.

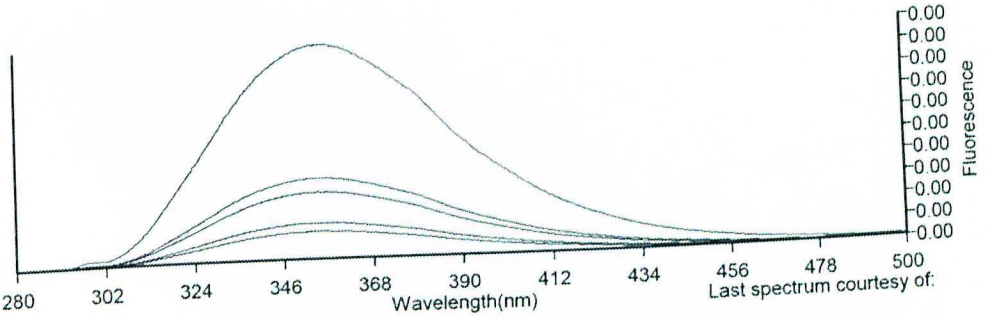

Supplemental Figure 5.3 Chart of the absorbance/ emissions of tyrosine and absorbance/ emissions of tryptophan. The program PhotoChemCad2.1 could not perform a simulated FRET interaction between the two residues, regardless of proximity, angle, and other parameters.